SOME INTERFACIAL STUDIES ON THE RUTILE-WATER DODECANE-SODIUM MYRSTATE SYSTEM

By
AMBRISH BHARGAVA

DEPARTMENT OF METALLURGICAL ENGINEERING
INDIAN INSTITUTE OF TECHNOLOGY KANPUR
AUGUST, 1973

SOME INTERFACIAL STUDIES ON THE RUTILE-WATER DODECANE-SODIUM MYRSTATE SYSTEM

A Thesis Submitted
In Partial Fulfilment of the Requirements
for the Degree of
MASTER OF TECHNOLOGY

By
AMBRISH BHARGAVA

to the

DEPARTMENT OF METALLURGICAL ENGINEERING
INDIAN INSTITUTE OF TECHNOLOGY KANPUR
AUGUST, 1973

ME-1973- M- BHA-SOM

CERTIFICATE

Certified that the work 'Some Interfacial Studies on the Rutile - Water - Dodecane - Sodium Myristate System' has been carried out under my supervision and the same has not been submitted elsewhere for a degree.

A. K. Biswas

(A. K. Biswas)
Associate Professor
Dept. of Metallurgical Engineering
Indian Institute of Technology
Kanpur

ACKNOWLEDGEMENTS

The author wishes to express his deep sense of gratitude to Dr. A.K. Biswas who guided this work to completion and contributed uncountable suggestions and criticism during the course of this work.

I am greatly indebted to my colleagues, Shri V.K. Bansal, Shri R.K. Malik, Shri N.B. Ballal and J.L. Modi without whose regular ungrudging assistance, the work would not have completed in time.

The technical assistance of Shri S.P. Nigam of Physics Department, Shri S.C.D. Arora of Metallurgy Department and typing work by Shri J.K. Misra are also thankfully acknowledged.

Lastly the cooperation of all my friends and well wishers is gratefully acknowledged.

AMBRISH BHARGAVA

TABLE OF CONTENTS

LIST OF TABLES

Figure Page

SYNOPSIS

Adsorption of Na-Myristate has been studied in the system rutile water dodecane. The distribution of Na-myristate between water and dodecane was measured as a function of pH. The effect of this surfactant on the water - dodecane interfacial tension has also been measured. Adsorption of Na Myristate at the rutile water interface has been found to be much smaller than at the rutile - dodecane interface.

In the pure 3 phase system the contact angle is found, to be zero. Addition of Na - Myristate resulted in finite contact angles, the contact angles were found to be very sensitive to the concentration of Na-Myristate and the pH.

The relationship among adsorption, interfacial tensions and contact angles was investigated and established in terms of the order of magnitudes.

A quantitative determination of the adsorption magnitude at the 3-phase interface and the subsequent interfaces was attempted, but the attempt was not successful owing to the experimental difficulties and the use of a weak β-emitter namely C_{14} Myristic acid.

CHAPTER I

INTRODUCTION

Flotation is characterized by the establishment of contact among three phases. In froth flotation these phases are the solid to be floated, an aqueous electrolyte solution, and a gas usually air. This gaseous phase may be replaced by an organic liquid phase[1]. Essentially the understanding of the flotation systems is based on the understanding of the phenomena at the three interfaces which separate these three phases.

The collectors used in flotation processes are heteropolar surface active agents, adsorbed from dilute solutions on the interfaces characterizing a solid-liquid-gas or solid-water organic liquid system. Simultaneous adsorption on the three interfaces in a three phase system and the quantitative determination of the adsorption density has lately received tremendous amount of attention because such studies are crucial for understanding the process of accumulation of mineral particles in the water-air (flotation) or water-organic liquid interface.

I.1 Young's Equation and Contact Angles[1,2,3]:

The thermodynamic condition for stable equilibrium of the three phases which are separated from one another by a contact line is expressed by the Young equation.

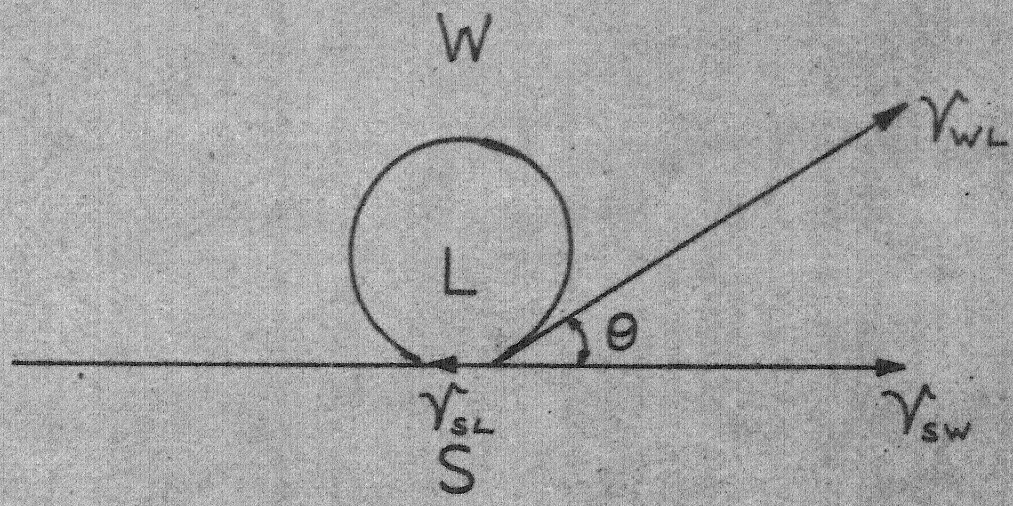

$\gamma_{SL}, \gamma_{WL}, \gamma_{SW}$: interfacial tensions.

W : water S : solid.

L : organic liquid.

θ : contact angle.

Fig.1. equilibrium interfacial tensions.

$$\gamma_{SL} - \gamma_{SW} = \gamma_{WL} \cos \theta_c \qquad (1.1)$$

where,

γ_{SL} = Interfacial tension between solid/organic liquid phase,

γ_{SW} = Interfacial tension between solid/water phase,

γ_{WL} = Interfacial tension between water/organic liquid phase, and

θ = [illegible] contact angle measured across the water phase in the system solid-water-liquid (organic).

The Young equation is valid only under equilibrium conditions and if the solid is non-deformable. If a solid phase is deformable, i.e. has a Young's Modulus below 10^{10} dynes/cm. as will be the case for rubber and certain gels, the Young equation will be invalid.

In order to have a stable contact it follows from equation (1.1) that the inequality.

$$\gamma_{SL} - \gamma_{SW} \leq \gamma_{WL} \qquad (1.2)$$

must be satisfied otherwise the Young equation will give an imaginary value of θ. Since the Young equation is applicable only to equilibrium systems, it is important to note that the surface tensions expressed in equations (1.1) and (1.2) refer to the boundaries between three phases, mutually saturated with respect to one another.

If water completely wets the solid surface, then,

$$\gamma_{SL} - \gamma_{SW} > \gamma_{WL} \qquad (1.3)$$

and the organic liquid phase is separated from the solid not by an adsorbed film but by a macroscopically thick layer of water and the contact angle is zero. Both the equations (1.2) and (1.3) are important in flotation or equivalent systems (whether the third phase is air or organic liquid).

I.2 Interfaces (Solid/Liquid, Liquid/Gas or Organic Liquid, Solid/Gas or Organic Liquid):

To increase the magnitude of the contact angle, or to establish a finite contact angle in the case of solids which are completely wetted by water, the difference $(\gamma_{SL} - \gamma_{SW})$ must decrease.

The Young equation (1.1), gives no information as to the changes in the surface tension of the three interfaces. This information may be obtained from the Gibbs Adsorption Equation formulated for each interface. From thermodynamic reiterations it is postulated that

$$d\gamma = -S^{\Delta} dT - \Sigma \Gamma_i \, d\mu_i \qquad (1.4)$$

where,

γ = intensive thermodynamic property of a two phase system called surface tension,

S^{Δ} = surface entropy

Γ_i = Adsorption density of the i-th adsorbed species,

μ_i = chemical potential of the i-th species.

Since we are mainly interested in constant temperature and pressure processes, the Gibbs equation when applied to flotation system becomes,

$$d\gamma = -\Sigma \Gamma_i \, d\mu_i \qquad (1.5)$$

Therefore the adsorption density of the i-th component relative to that of component 1 is defined by the relation,

$$\Gamma_i = \left[\frac{\partial \gamma}{\partial \mu_i} \right]_{T,\ \text{all}\ \mu\text{'s except}\ \mu_i\ \text{and}\ \mu_1}$$

or introducing the activity term,

$$\Gamma_i = -\frac{1}{RT} \left(\frac{\partial \gamma}{\partial \ln a_i} \right)_{T,\text{all}\ \mu\text{'s except}\ \mu_i\ \text{and}\ \mu_1} \qquad (1.6)$$

If very dilute solutions are being dealt with, then activity coefficient terms are approximated to be unity.

However, some experimental workers have also employed a constant and large concentration of neutral electrolyte, so that small variations of concentrations in dilute surfactant solutions do not alter the activity coefficient terms.

$$\Gamma_i = -\frac{1}{RT} \left(\frac{\partial \gamma}{\partial \ln C_i} \right)_{T,\ \text{all}\ \mu\text{'s except}\ \mu_i\ \text{and}\ \mu_1.} \qquad (1.7)$$

Solid/liquid and solid/gas interfaces changes in interfacial tension cannot be measured directly but may be obtained from adsorption density measurements as a function of concentration. A plot of Γ_i vs. C_i is referred to as Adsorption Isotherm.

From (1.7),

$$d\gamma = - RT \Gamma_i \; d \ln C_i \qquad (1.8)$$

Area under the curve of a plot of Γ_i vs $\ln C_i$ between the limits C_1 and C_2 gives the value of $\Delta\gamma$, between $C_1 - C_2$, using the usual notations,

$$\Delta\gamma_{SW} = - RT \int_{C_1}^{C_2} \Gamma_{SW} \, d \ln C \qquad (1.9)$$

$$\Delta\gamma_{SL} = - RT \int_{C_1^*}^{C_2^*} \Gamma_{SL} \, d \ln C \qquad (1.10)$$

Now from (1.1),

$$\Delta\gamma_{SL} - \Delta\gamma_{SW} = \Delta\gamma_{WL} \cos \theta_e \qquad (1.11)$$

Substituting (1.9) and (1.10) in (1.11),

$$- RT \left[\int_{C_1}^{C_2} \Gamma_{SL} \, d \ln C - \int_{C_1^*}^{C_2^*} \Gamma_{SW} \, d \ln C \right] = \Delta\gamma_{WL} \cos \theta_e \qquad (1.12)$$

De Bruyn, Overbeek and Schuhmann[4] in 1954 showed by a thermodynamic analysis of the three phase flotation system that if a solid were to become floatable the adsorption density of the collector at the solid/gas interface must exceed the adsorption density of the collector at the solid/liquid interface. A quantitative confirmation of the prediction made by De Bruyn et al was given by Smolders[5] in 1961 for the system, Mercury/Aqueous solution

of sodium-decyl sulfonate/hydrogen gas. In this system it is possible to determine experimentally the surface tension of all three interfaces. The slope of the γ - log concentration curve was a direct measure of the adsorption density and it was found that at all concentrations, $d\gamma / d \log C$ is greater for the Hg/gas than for the Hg/liquid interface. He also pointed out that the measured contact angles are in good agreement with the contact angles calculated from the Young equation combined with Gibbs Adsorption equation.

J.H. Schulman and J. Leja[6] in 1954 said that oil in water emulsions are stabilised by solid powder when contact angle is $\leq 90^{\circ}$. If contact angle is $\geq 90^{\circ}$ water in oil emulsions are promoted. Stabilisation can be achieved by low energy solids like talc etc. or hydrophilic solids coated with surfactants. The contact angle developed is the resultant effect of the density of coverage and the length of the hydrocarbon chain. Density of coverage depends upon the nature of solid surface, collector concentration, pH, polar group of surfactant etc, $BaSO_4$ water-benzene systems were investigated in presence of sodium oleate, dodecyl sulphate etc. The adsorption measurements were however not done.

Aplan and De Bruyn[7] (1963) supplemented the fact surfaced by De Bruyn[4] earlier, by experimentally determining the adsorption of Hexyl mercaptan on gold from the liquid and

the gas phase and concluded that adsorption on the solid/gas interface is higher than on the other interfaces. The adsorption at the solid/gas interface was measured by the Mc Ban balance for the system 'gold powder - aqueous solution of weakly dissociated collector - and a gaseous phase nitrogen saturated with respect to both water vapour and mercaptan vapour.

Mellgren and H.L. Shergold,[8] (1966), whilst dealing with the recovery of ultrafine mineral particles by extraction with an organic phase stressed the importance of the contact angles for the system quartz particles in water-iso-octane interface in presence of lauryl amine and found that extraction is higher with higher collector concentration and maximum at intermediate pH 6-8.

Deckker and Gaudin[9], worked on the system quartz-water-Dodecane modified by Dodecyl Amine as collector, and succeeded in establishing a relationship among adsorption, interfacial tensions and contact angles. The graphical integration method was used to determine the changes in the quartz/dodecane and quartz/water interfacial tensions as a function of amine concentration at constant pH and ionic strength.

Somasundaran[10] (1968), studied the system quartz-water-air, and used DDAA as collector. He also found by using the adsorption data of Li (Ph.D. Thesis, M.I.T.) and determining the adhesion tension $\gamma_{LG} \cos \theta$; that the

adsorption at the solid/gas interface is greater than at the two interface. Actual measurements at solid/gas interface were not made.

A correlation was made by Shergold and Mellgren[11], (1969) between the percentage of hematite concentrated, the extent of adsorption, electro-kinetic properties and the contact angles between the three phases, in the system, hematite iso-octane-water with Dodecyl sulphate.

It was found that 100 percent of hematite was concentrated at the oil water interface when the hematite zeta potential was zero. Adsorption density was measured from the aqueous phase and not from the organic phase. A semi-theoretical equation was deduced stating that $\Delta\zeta$ is proportional to the adsorption density.

Shergold and Mellgren[12] extended their work to find the distribution of amine between the organic and the aqueous phase. Adsorption density was calculated only from the aqueous phase, the work of adhesion

$$W_a = \gamma_{ow} (1 - \cos\theta) \qquad (1.13)$$

was determined and 100 percent recovery of quartz was reported when equilibrium aqueous amine concentration are such that ζ potential is zero and contact angle is around 90°.

The presence[13] of large amounts of neutral amine in the organic phase produced higher contact angles. This effect was however, dependent on the presence of cationic amine in the aqueous phase. In alkaline solutions, the contact angles, work of adhesion, percent recovery and adsorption density decreased rapidly as a function of concentration. The decrease in these variables correspond to a decrease in the cationic amine concentration. Hematite was never completely wetted by the oil phase.

Lin and Metzer[14], (1972) presented a method based on the measurement of surface tensions and contact angles as a function of collector concentration, by which the quantitative adsorption at the 3-phase interface can be determined.

$$\Gamma_{SG} = -\frac{\gamma_{LG}}{\beta RT}\frac{d\cos\theta}{d\ln C} + \Gamma_{SL} + \Gamma_{LG}\cos\theta \qquad (1.14)$$

where,

Γ_{SL} = adsorption density at the solid gas interface,

γ_{LG} = interfacial tension at the liquid/gas phases,

R = universal gas constant,

β = constant,

T = temperature in ^{o}K,

C = equilibrium concentration of the collector in aqueous solution,

θ = contact angle measured in the aqueous phase

Γ_{SL} = adsorption density at S/L interface, and

Γ_{LG} = adsorption density at L/G interface.

I.3 Distribution Coefficient:

The distribution coefficient at a particular collector concentration and pH gives the relative amounts of material in the organic phase and the aqueous phase[12].

$$K_D = \frac{\text{Total Fatty Material in Organic Phase}}{\text{Total Fatty Material in Aqueous Phase}}$$

$$= \frac{|RCOOH|_o}{|RCOO^-|\ |RCOOH|_a} \qquad (1.15)$$

where,

K_D = apparent distribution coefficient,

$|RCOOH|_o$ = fatty acid in organic phase,

$|RCOOH|_a$ = fatty acid in aqueous phase.

From equation (1.6) it is possible to calculate the actual distribution coefficient which is defined as

$$D = \frac{|RCOOH|_o}{|RCOOH|_a} \qquad (1.16)$$

Powney and Jordon[15] have published data on the hydrolysis of sodium salts of fatty acids where from it is possible to come down to equation (1.7) as has been shown by Dixit and Biswas[16]. A detailed reiteration is made elsewhere in the text.

1.4 Autoradiography and Tracer Techniques:

Microautoradiography as introduced by Plaskin[17] in 1957 is a technique whereby the mineral surface under investigation is conditioned with a solution of beta labelled collector, washed dried and contacted with a beta-sensitive emulsion, which gives a auto-radiogram. This is utilised in predicting many a complex problems of the mineral surfaces. The analysis of a auto-radiogram is accomplished by a photometer, which relates the transmittance to the contours of the material adsorbed on the interface.

Plaskin and Shafeyev[18] in 1957 with the help of the autoradiograms for the distribution of xanthate on the surface of sulphide minerals were able to predict the heterogenity of the distribution of the xanthate over the mineral surface, and explained this by saying that the sulphide mineral surface is not equi-potential.

From Plaskin's work the line was towed by many workers, to establish a direct method of measuring the adsorption densities at the various interfaces and at the three phase interface where the adsorption density is said to be maximum. Mazumdar and Vishwanathan[19], have towed the line and have established in terms of count rate that the maximum adsorption occurs at the 3-phase interline, which is consistent with Klasseen's work[19].

(a) Tracer Techniques:

Radioactive isotopes are profitable research tools available for studying the diversified and complex problems arising in the dressing of minerals. Indeed, Taggart[20] has observed that their applicability is limited only by the imagination of the investigation. The use of radioactive isotopes as a scientific tool is not new, but it is only in the last few years that they have been made available in quantity and at a reasonable cost.

The instruments normally employed to detect the ionizing events produced in gases on exposure to radiation are ionization chambers, proportional contours and Geiger[23] Muller counters. The end window type Geiger Muller counter has been used frequently in mineral dressing investigations.

Tracer technique measurement of adsorption at the S/L interfaces have been widely discussed[21-26]. But the literature on simultaneous adsorption at the interfaces of the 3-phase system is scanty.

Mazumdar and Vishwanathan[19] of BARC have measured the radiations coming from a solid surface, where a three phase contact had been established. This was accomplished by using a series of concentric lead discs of varying diameters which were used to mask the unwanted areas.

1.5 Philosophy of the Problem:

In view of increasing importance of flotation practice and the technological possibility regarding the process of accumulation of ultrafine mineral powders at the water/organic liquid interface, it is desirable to understand the adsorption behaviour of collectors at the various interfaces and to seek a correlation between the contact angles, interfacial tensions and the magnitude of adsorption on solid surface from both aqueous and organic liquids. A study of the distribution of the collector between the two phases is called for prior to subsequent adsorption, interfacial tension and contact angle studies. Rutile-water-dodecane-myristic acid and its sodium salt offers itself as a convenient system for detailed study.

From the literature, it is clear that very few workers have measured the magnitude of adsorption of collector from the organic liquid phase although the importance of contact angle, interfacial tension and zeta potential studies have been stressed.

Investigations on the chosen system pursued on the following lines, were considered useful towards elucidation of fundamentals regarding the technological process mentioned earlier.

(1) Study on the distribution coefficient of sodium myristate between the dodecane and the water phase, varying the Na-myristate concentration in the aqueous phase and pH.

(2) Contact angle and interfacial tension studies varying the collector concentration and the pH.

(3) Adsorption studies with reference to variation of pH in the water phase and the collector concentration in both organic liquid (dodecane) and water phase.

(4) Direct measurements of adsorption magnitudes at the three phase interline as a function of pH and concentration of sodium myristate.

(5) Correlation of the adsorption, contact angle and interfacial tension studies with particular reference to adhesion tension and changes in solid-liquid interfacial tensions as computed through the use of Gibbs adsorption equation.

(6) Prediction of optimum conditions for recovery of rutile slime in the water-dodecane interface using sodium myristate as collector.

CHAPTER II

MATERIALS

In the present work aimed at studying the interfacial phenomenons. Rutile-water-dodecane system has been selected as dodecane is almost insoluble in water and the three represent stable phases.

The collector used throughout the course of experiments was sodium-myristate ($C_{13}H_{27}COONa$). The details of the chemicals and the materials used are mentioned below.

2.1 Titanium Dioxide (TiO_2):

The sample of rutile (TiO_2) powder was procured from May and Baker Ltd., Dagenham, England. The estimated purity was greater than 98 percent and contains not more than 0.5 percent water soluble substances.

2.2 Collector:

Sodium-myristate was used as collector throughout the course of the experiments.

Myristic Acid:

The untagged myristic acid was obtained from the Hormel Institute fatty acid project at University of Minnesota, USA. Estimated purity was > 99 percent as determined by gas-liquid and then layer chromotography analysis. Properties of myristic acid are listed in Table 1.

Preparation of Sodium Myristate:

The procedure followed was similar to that of Kajiji[32]. Equivalent amounts of myristic acid and analytical grade sodium hydroxide were transferred to a round bottom flask and 50 ml. of dry absolute alcohol was added. The ethyl alcohol used had been distilled, kept overnight over quick lime and redistilled.

The whole mass was reflexed over a water bath for about an hour. Subsequently, excess alcohol was removed by evaporation and syrupy mass was poured hot in acetone which had been distilled after keeping overnight with $CaCl_2$. Sodium myristate thus precipitated was filtered and washed with acetone. The dried powder was stored in a cool dry place.

Labelled Myristic Acid:

The labelled myristic acid was obtained from isotope division of Bhabha Atomic Research Centre, Bombay. The specific activity of the acid is reported to be 3.27 mC_i/m.mole. The labelled myristic acid was obtained in solid form and was dissolved in benzene.

2.3 n-Dodecane:

The sample was procured from BDH Chemicals Ltd., Poole, England, estimated purity was greater than 99 percent as determined by gas-liquid chromatography. n-dodecane was

distilled at 215°C, and the residue left behind was rejected. The properties of n-dodecane are listed in Table 2.

2.4 Rutile Single Crystal:

A synthetic rutile crystal supplied by the Linde Co., Chicago, USA was used. It was cylindrical in shape 1/2 in. diam., with faces cut perpendicular to the C-axis. The crystal has been stated to be alumina free and 99.9 percent pure. Rutile is a high surface energy solid its calculated average field strength being 2.7×10^5 e.s.u.[33].

2.5 Other Chemicals:

Other chemicals used for analytical purpose were all of analytical grade. Rhodamine 6G used was supplied by BDH, England.

CHAPTER III

EXPERIMENTS AND RESULTS

In the present work, distribution of sodium myristate, contact angle, interfacial tension and adsorption measurements have been done. In this chapter the experimental techniques are described briefly and the experimental results are presented.

3.1 Critical Micelle Concentration Measurement:

a) Conductivity Technique:

The conductivity was measured in 'Kundoktometer E-382' model apparatus. The cell constant of the conductivity cell was 0.8172 cm^{-1}. The measurements were done at a constant temperature of 25 $\pm$ 0.1°C tripple distilled water of conductivity 1 x 10^{-6} to 2 x 10^{-6} mhos.cm^{-1} was used for all conductivity measurement.

b) Colorimetric Technique:

Critical micelle concentration of sodium myristate was determined by the colorimetric (dye titration) method of Corrin and Harkin.[27]

The change of color from fluorescent greenish red to non fluorescent red corresponds to the c.m.c. of sodium myristate. This change in color is due to preferential solublization of one of the tautomeric forms of the dye within the interior of soap micelles. The absorbance value was measured at 415 mμ.

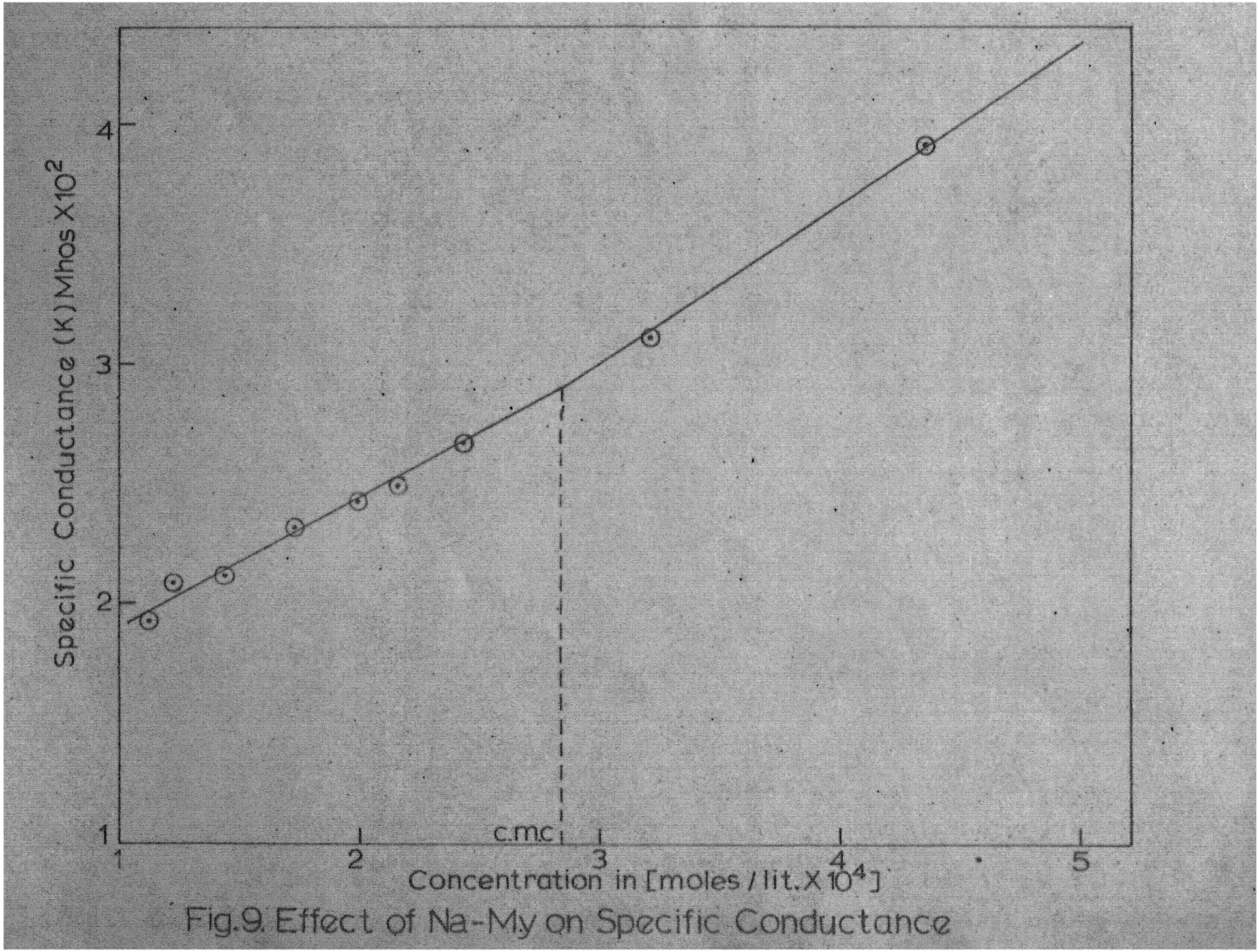

Fig.9. Effect of Na-My on Specific Conductance

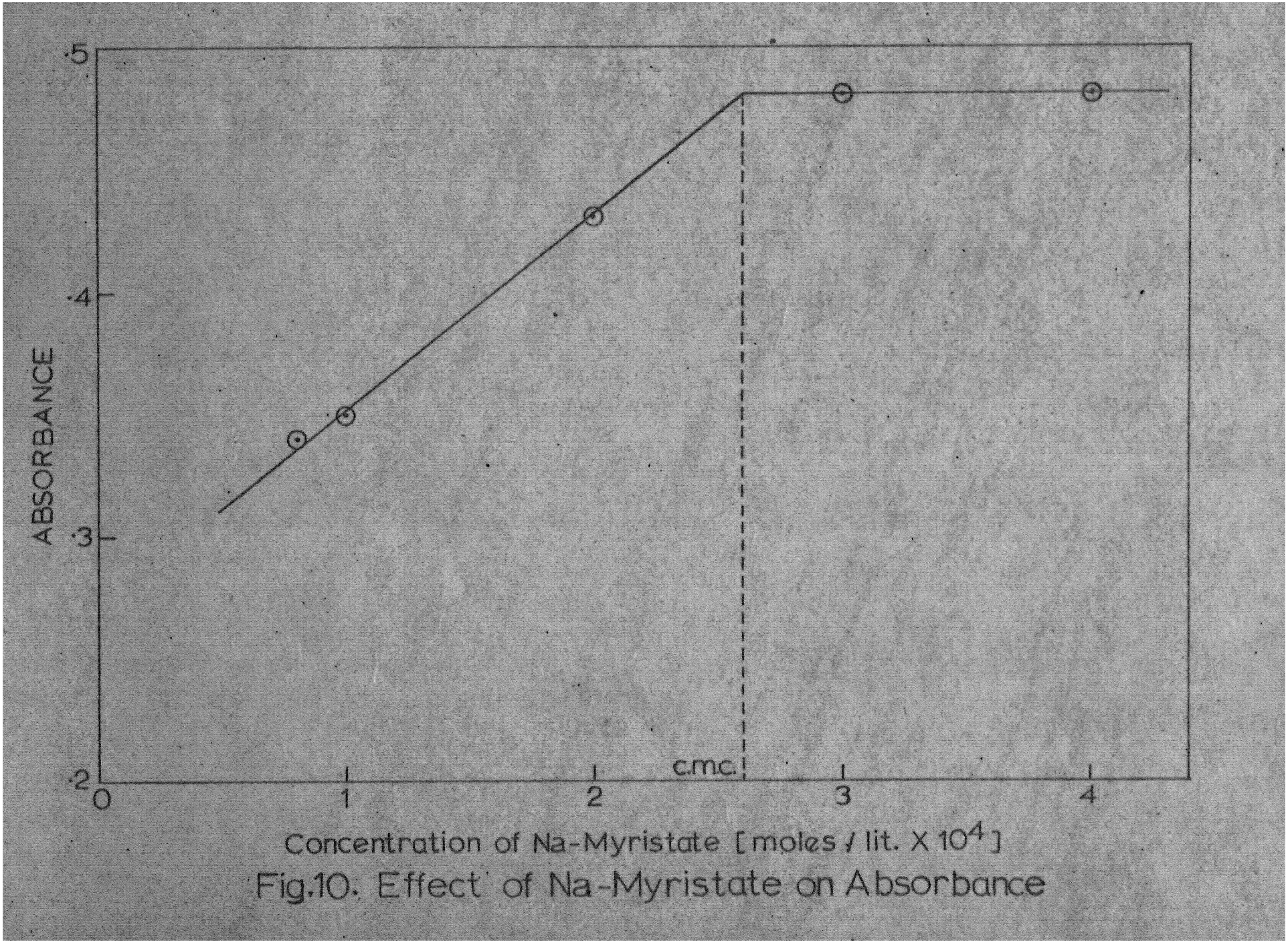

Fig.10. Effect of Na-Myristate on Absorbance

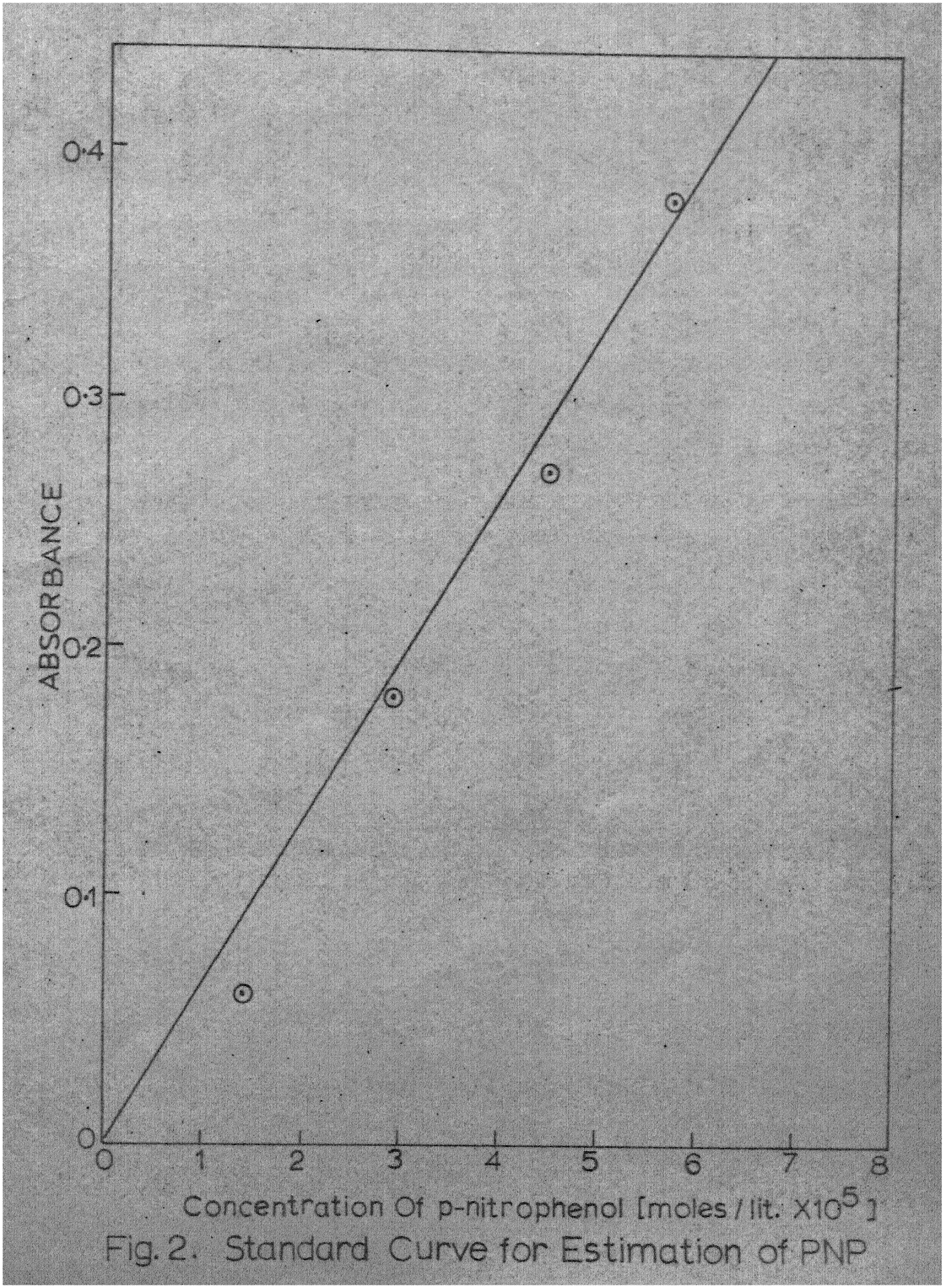

Fig. 2. Standard Curve for Estimation of PNP

This change in color was determined by the abrupt increase in absorbance value of the solution using spectronic 20 colorimeter. The corresponding concentration at which the absorbance value abruptly increases gives the c.m.c. value of sodium myristate.

The results of specific conductance measurements (Fig. 9), Table 3) show a sharp increase in the specific conductance of water at a Na-myristate concentration of 2.84×10^{-4} (moles/lit), which determines the c.m.c. of Na-myristate.

The absorbance values of sodium myristate has been shown in Fig. 10, Table 4. The sharp change in the absorbance value gives the c.m.c. of sodium myristate. The c.m.c. value of sodium myristate by this technique is found to be 1.6×10^{-4} (moles/lit.).

The c.m.c. values obtained from (a) conductivity measurements, (b) colorimetric measurements came out in a close agreement to the c.m.c. value of 2.9×10^{-4} moles/lit. published by Powney and Addison[29].

3.2 Surface Area Determination of TiO_2 Sample:

The surface area of the rutile sample was measured by adsorbing p-nitrophenol on the rutile surface, as described by Giles.[30] One gram of dry rutile powder was taken in different polythene bottles and 20 ml. of aqueous p-nitrophenol solutions of different concentrations were

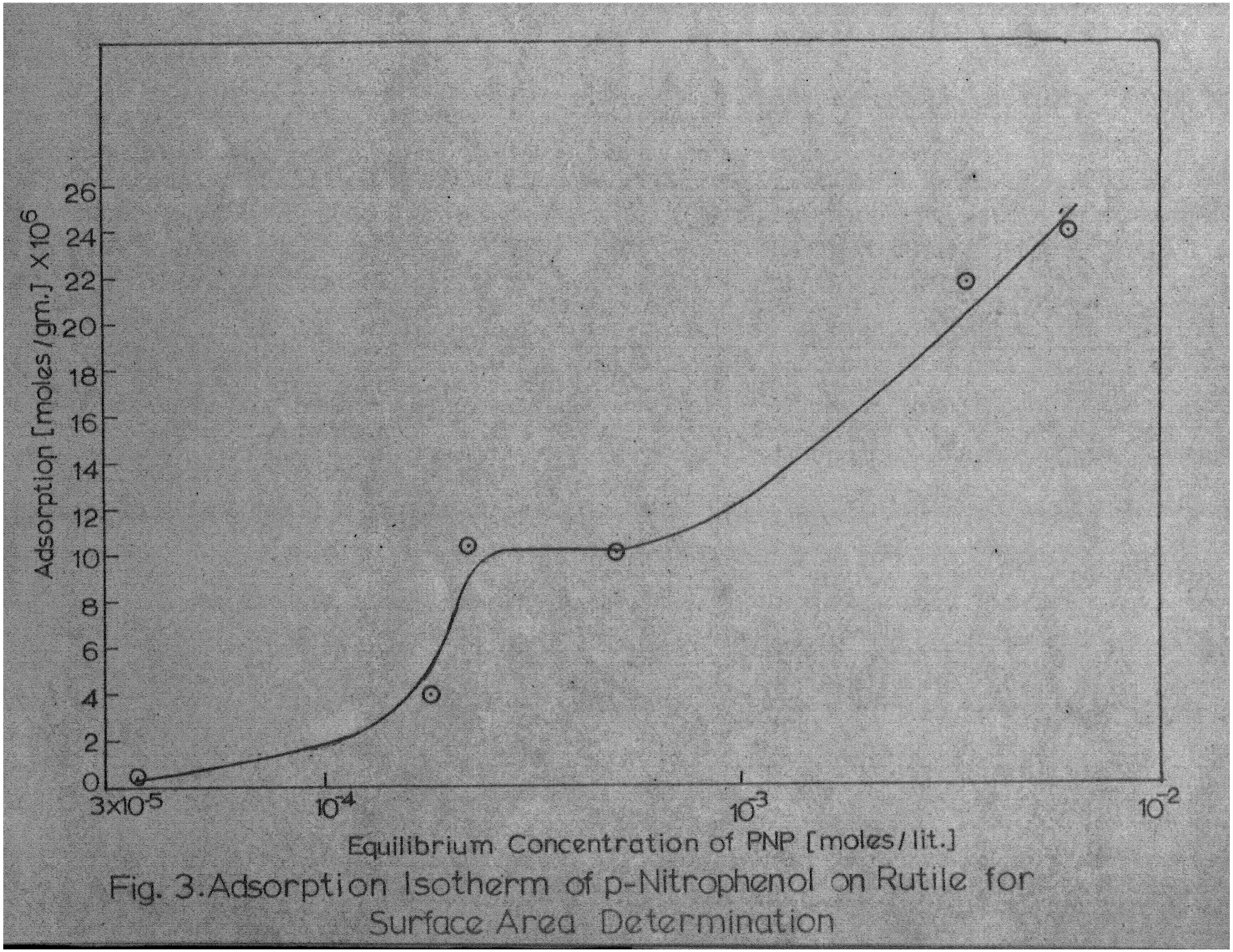

Fig. 3. Adsorption Isotherm of p-Nitrophenol on Rutile for Surface Area Determination

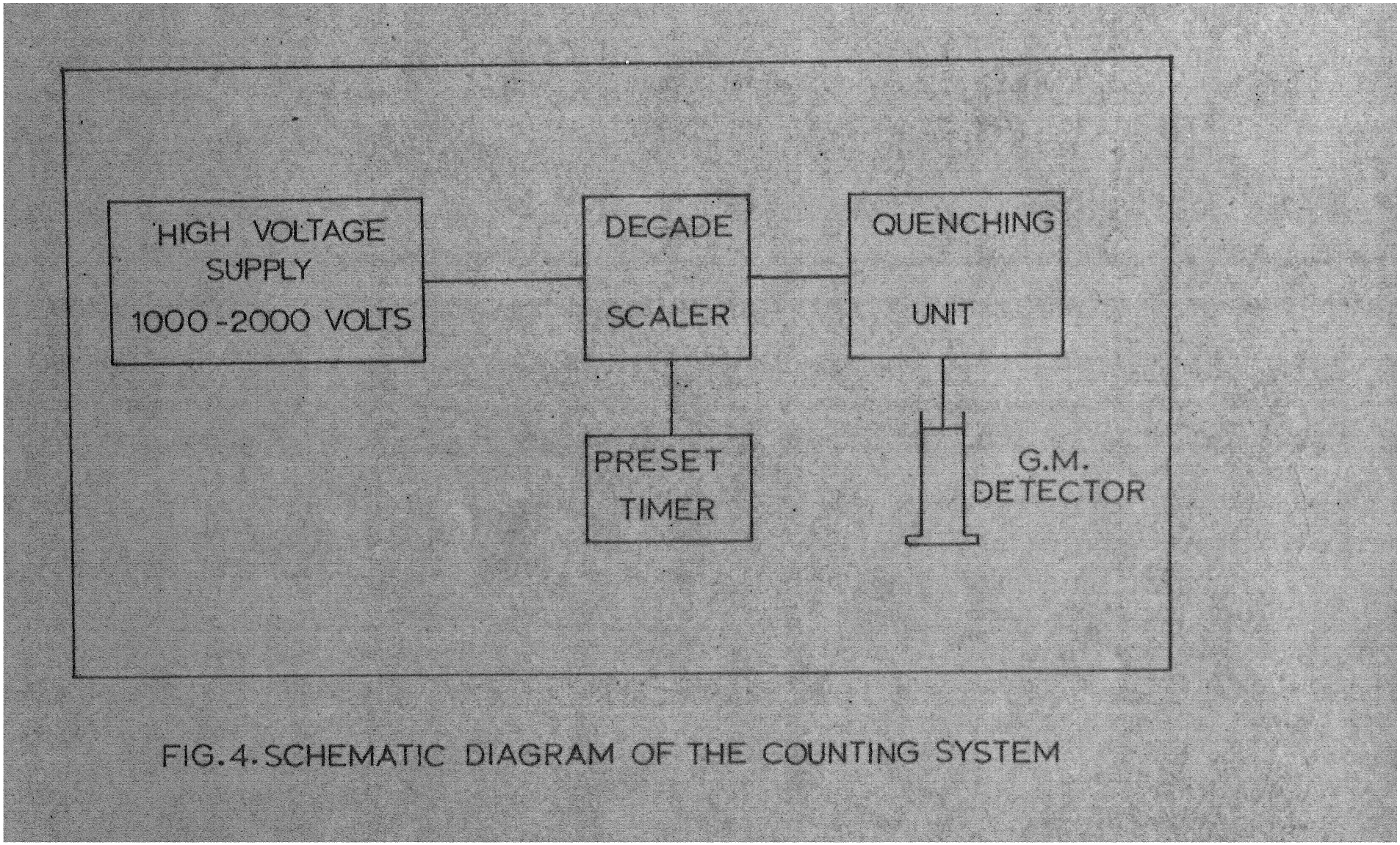

FIG. 4. SCHEMATIC DIAGRAM OF THE COUNTING SYSTEM

transferred to each of the bottles. The bottles were vigorously shaken and later kept in a thermostat at 30 ± .1°C for about six hours. The supernatent liquid was analysed colorimetrically using the standard curve shown in Fig.2. The pH was maintained at all times at 7.00 ± 0.1 and the absorbance was measured at 400 mμ.

The adsorption isotherm so obtained is given in Fig. 3, and values in Table 3. From the platcau of the curve the surface area was calculated to be 1.53×10^4 cm^2/gm. The cross-sectional area of p-nitrophenol molecule was taken to be 25 $Å^2$ as per Giles' suggestion.

3.3 Tracer Technique for Sodium Myristate Estimation:

The tracer element carbon-14 used to label myristic acid is a weak β-emitter and has a half life of 5700 years. The maximum energy of β-range is 0.155 Mev and would penetrate a layer of 0.2 cm thick myristic acid. Most of the β-particles have less than this energy. Therefore, if a very thin layer of sodium myristate is formed on the planchet, the effect due to self-absorption can be minimised. The best results can be obtained if the count rate is high compared to background, geometry is reproducible and the counting device shows stable behaviour. In the present investigation the Geiger-Muller counting system (Type I-1030 of Electronic Corporation of India, Hyderabad) has been used. The whole system is schematically shown in Fig. 4. It consists

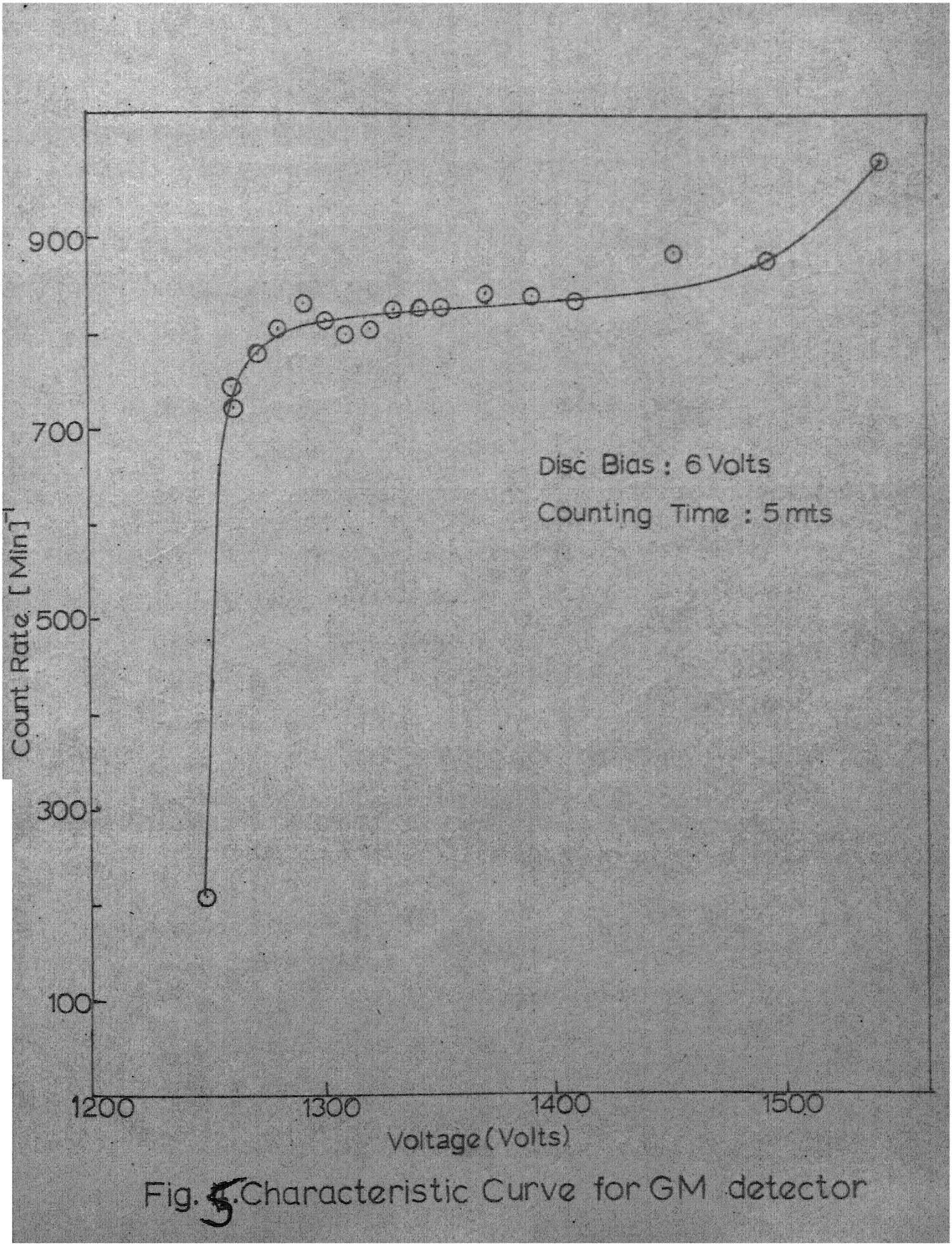

Fig. 5. Characteristic Curve for GM detector

of a high voltage supply (1000 volts to 2000 volts output), a preset timer capable of reading time accurately upto 0.1 secs. and a decade scaler to record the member of counts from the G.M. detector. The G.M. detector is mounted on a bakelite stand. The radioactive samples are taken in planchets (as described later) which is turn can be fitted into racks provided at various levels in the bakelite stand. A lead castle envelops the whole mounted assembly minimising the background.

Standardization of Conditions:

The optimum values of(a) voltage to be supplied to the central wire, and (b) disc. bias which depend on the noise level, have to be experimentally determined for a particular G.M. tube. As the voltage is increased from the threshold voltage at which the detector starts sensing the β-rays, the count rate increases in the initial stages. It then levels off for a fairly large range of voltage, again to start increasing at very high voltages (See Fig. 5). Wider the plateau, better is the performance of the detector. The change in count rate per 100 volt increase of voltage is taken as an index of the performance. The detector used in the present investigation showed an increase of 5 counts per min. for an increase of 100 volts (as specified by the manufacturers). Disc bias of 6 volts and filament voltage of 1250 volts were the optimum values for the present system,

as found with the help of standard C-14 β source. Depending on the concentration level the time for counting was kept between 10-30 minutes to obtain sufficiently large number of counts. Care was taken regarding background and geometry.

Radioactive C-14 labelled myristic acid had C-14 at the carbon of the carboxyl group and was procured from Bhabha Atomic Research Centre, Bombay. It was supplied in the solid form. This was then dissolved in benzine.

Preparation of Tagged Sodium Myristate Solution:

A suitable quantity (7 mg. was dissolved in 10 ml. of benzene and 0.02 ml was taken), of tagged myristic acid was transferred from the vial to a volumetric flask. Excess of sodium hydroxide solution was added to make the volume around 15 ml. The mixture was kept at 60°C for six hours in a thermostat with frequent shaking. The stopper was frequently opened to allow the benzene vapour to escape. At the end of this period, the saponification was assumed to be complete. The resulting solution was then added to a solution of untagged sodium myristate. The ratio of tagged to untagged was 1:170 and was maintained constant throughout the course of the experiments). The solution was stocked for further use.

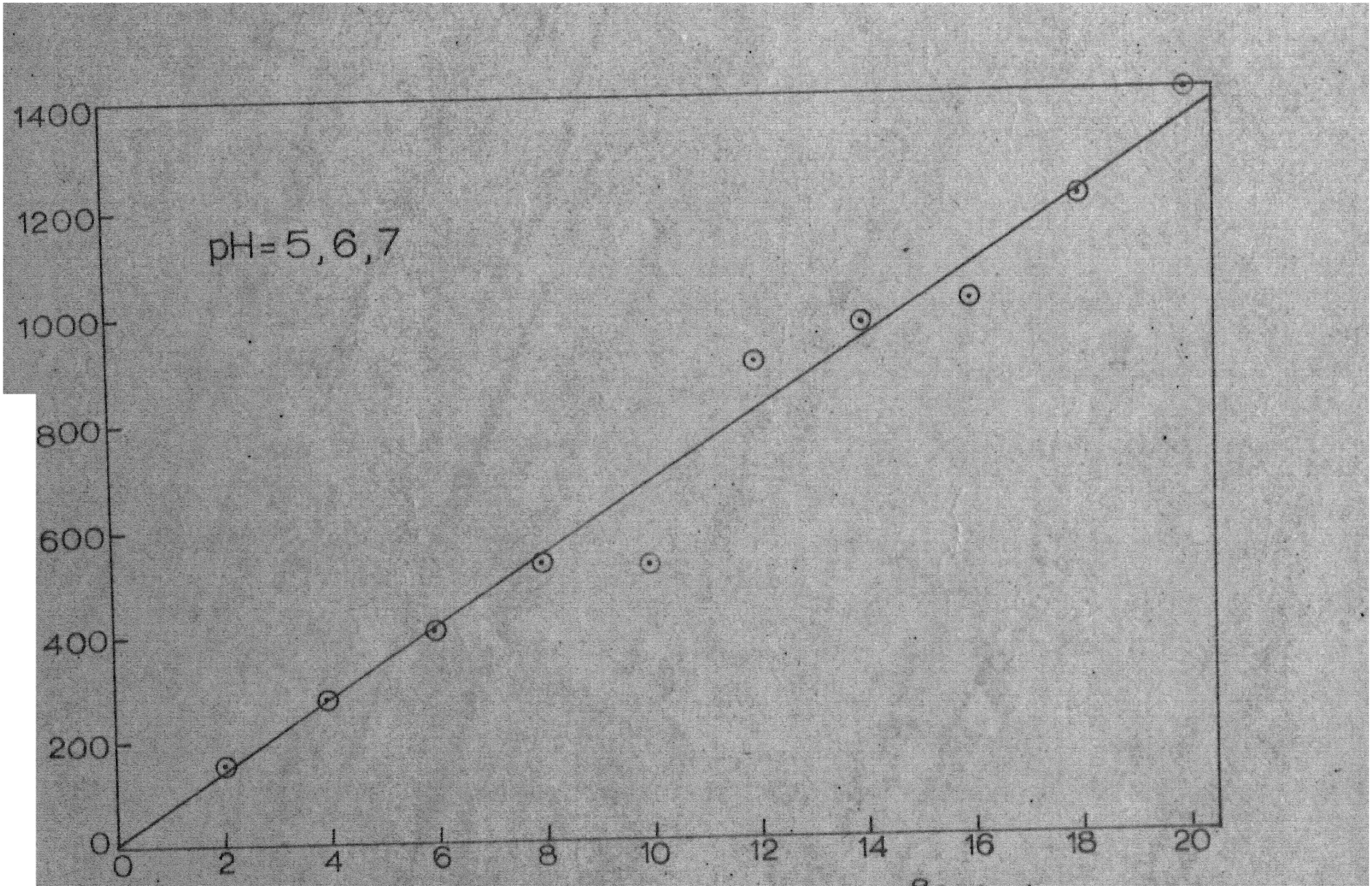

Fig.6. Standard Curve for Estimation of Sodium-Myristate by C_{14} Tracer

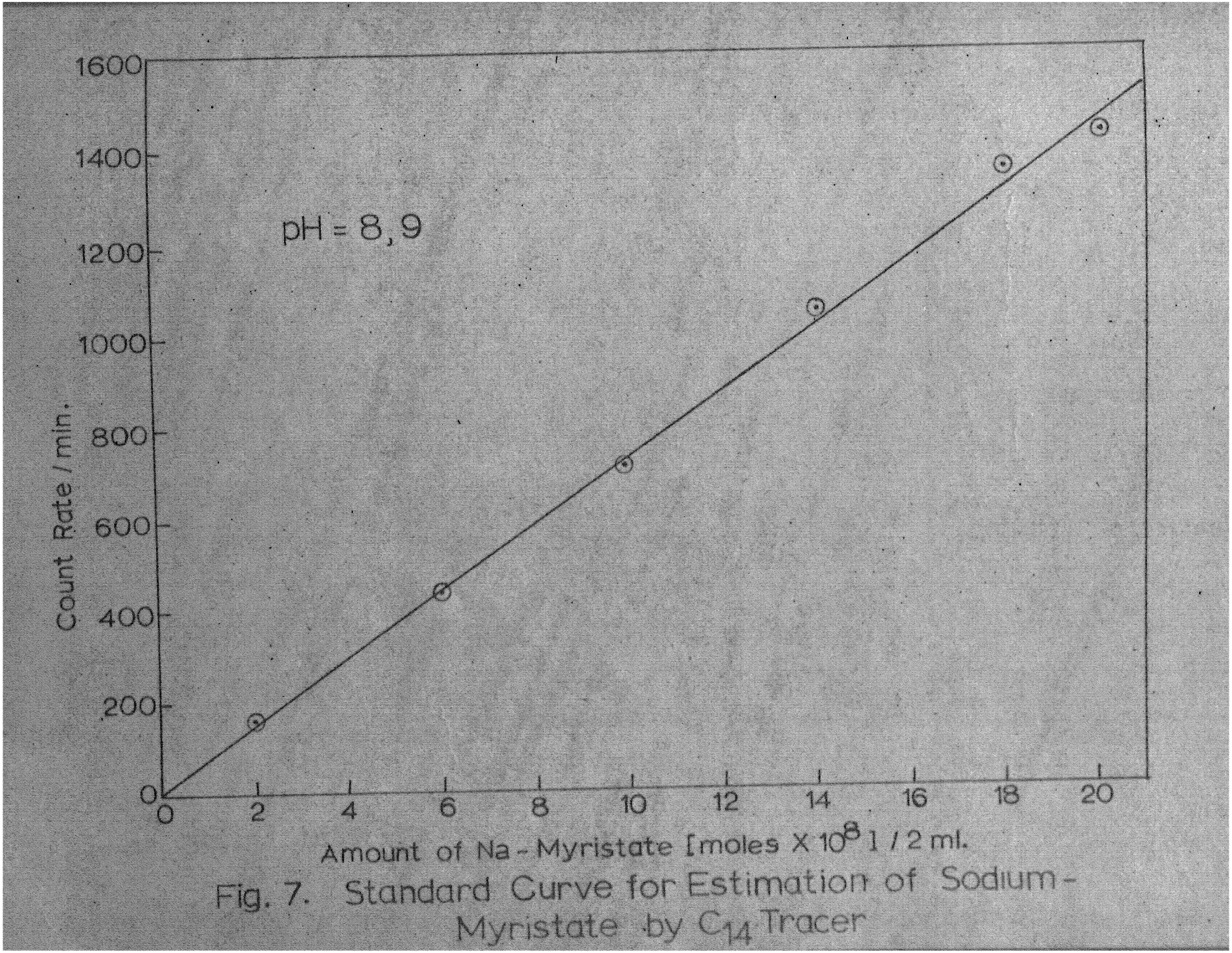

Fig. 7. Standard Curve for Estimation of Sodium-Myristate by C_{14} Tracer

Standard Curve:

Throughout the series of experiments, the experimental conditions like geometry of the sample holder, filament voltage etc. were kept unvaried. The perspex sample holders were circular in geometry and about 2/8" deep and could contain 2 ml. of liquid. Varying volumes of tagged sodium myristate (less than 2 ml.) were withdrawn from the stock solution and transferred to the planchet. To make the total volume 2 ml. the balance was made up by adding untagged sodium myristate solution of the same concentration to the planchet. The planchets were then kept at 40°C in an oven for about 10 hrs. This time was found sufficient for the water to evaporate. The planchet was then directly under the G.M. counter and the total number of counts were noted. Necessary background corrections were made. The standard calibration curve thus obtained is shown in Fig. 6,7 for different pH values and was used for estimation of solute in solutions of unknown concentrations.

3.4 Determination of Distribution Coefficient for Sodium Myristate Between Dodecane and Water:

Twenty ml of aqueous sodium myristate solution of varying concentration and containing previously mentioned proportion of tagged myristic acid were taken in different glass bottles to each of which 13 ml. of dodecane was added. The bottles were stoppered tightly and vigorously shaken for 1/2 hr. These were then kept at 30 ± 1°C for 6 hrs. for

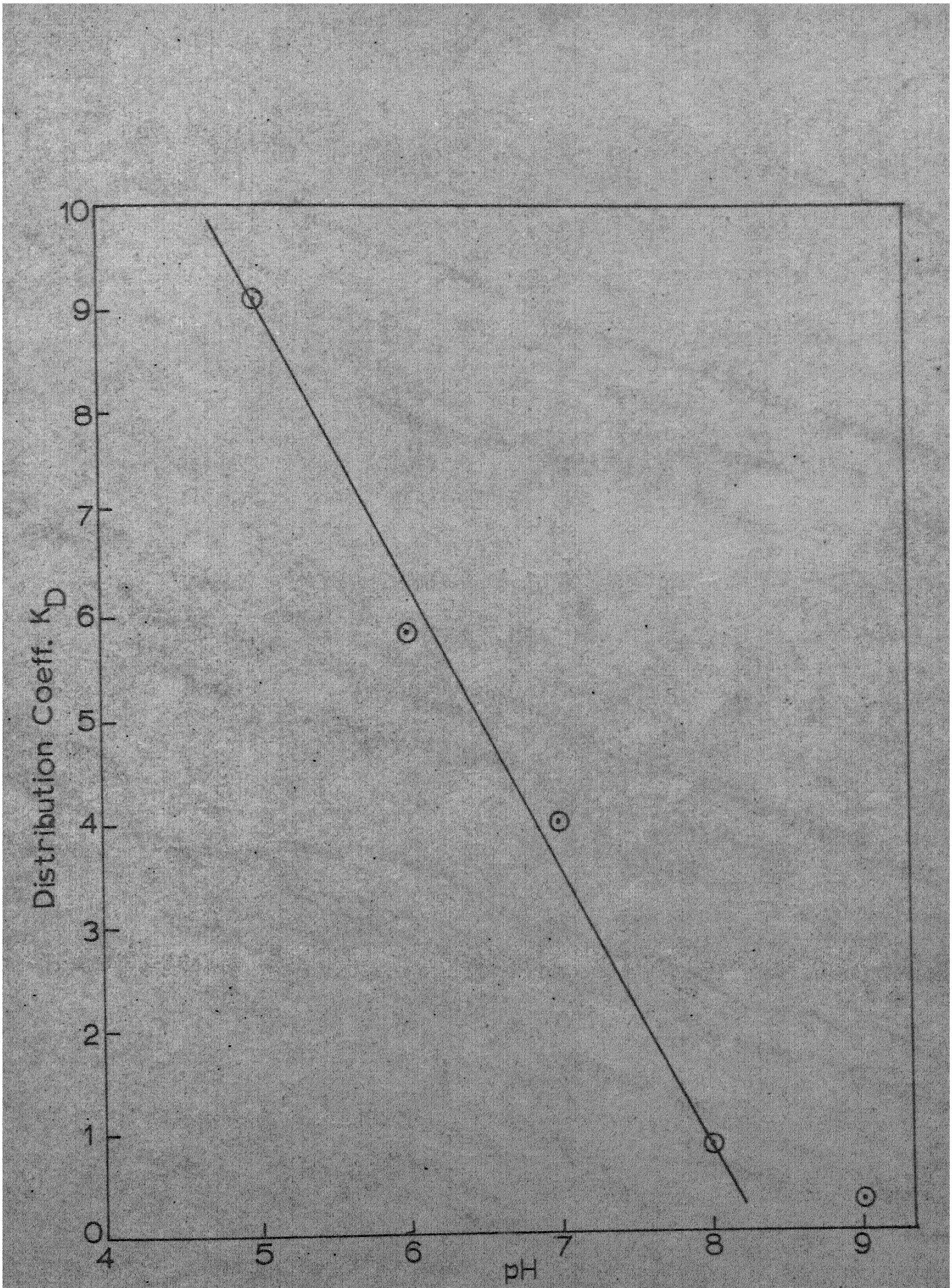

Fig.11. Effect of pH on Distribution Coeff. K_D

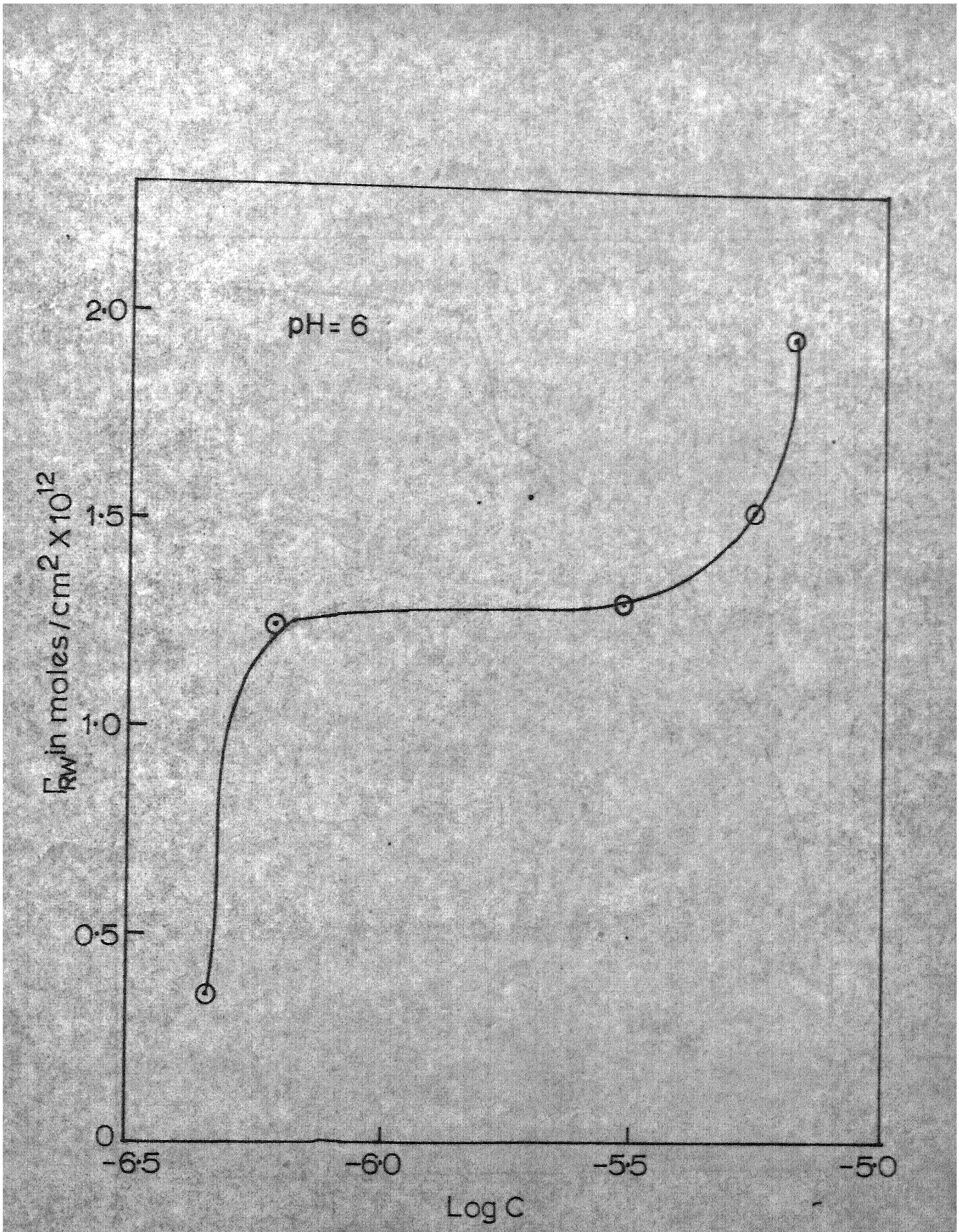

Fig.12. Adsorption Isotherm of Na-My on Rutile from water phase

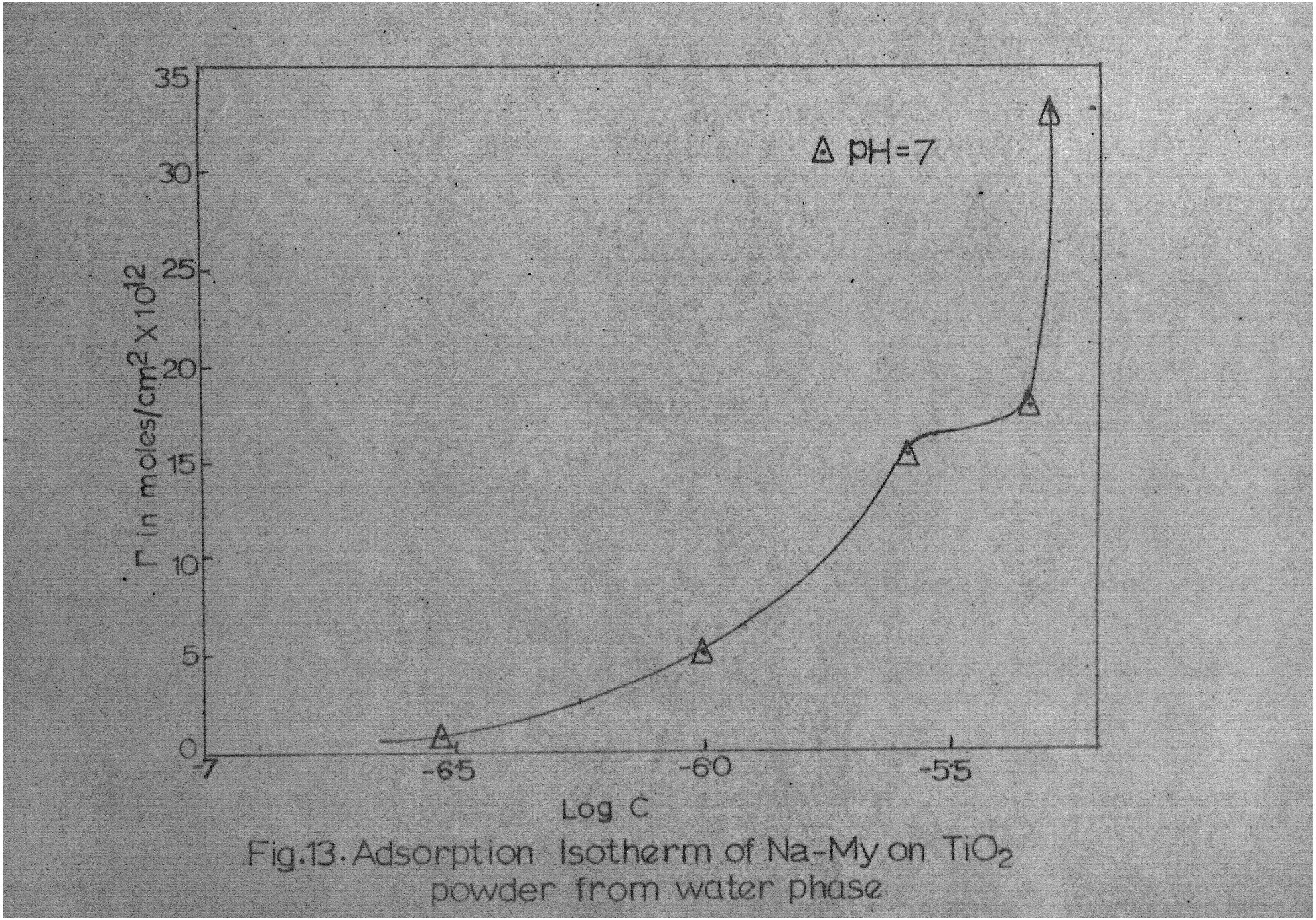

Fig.13. Adsorption Isotherm of Na-My on TiO_2 powder from water phase

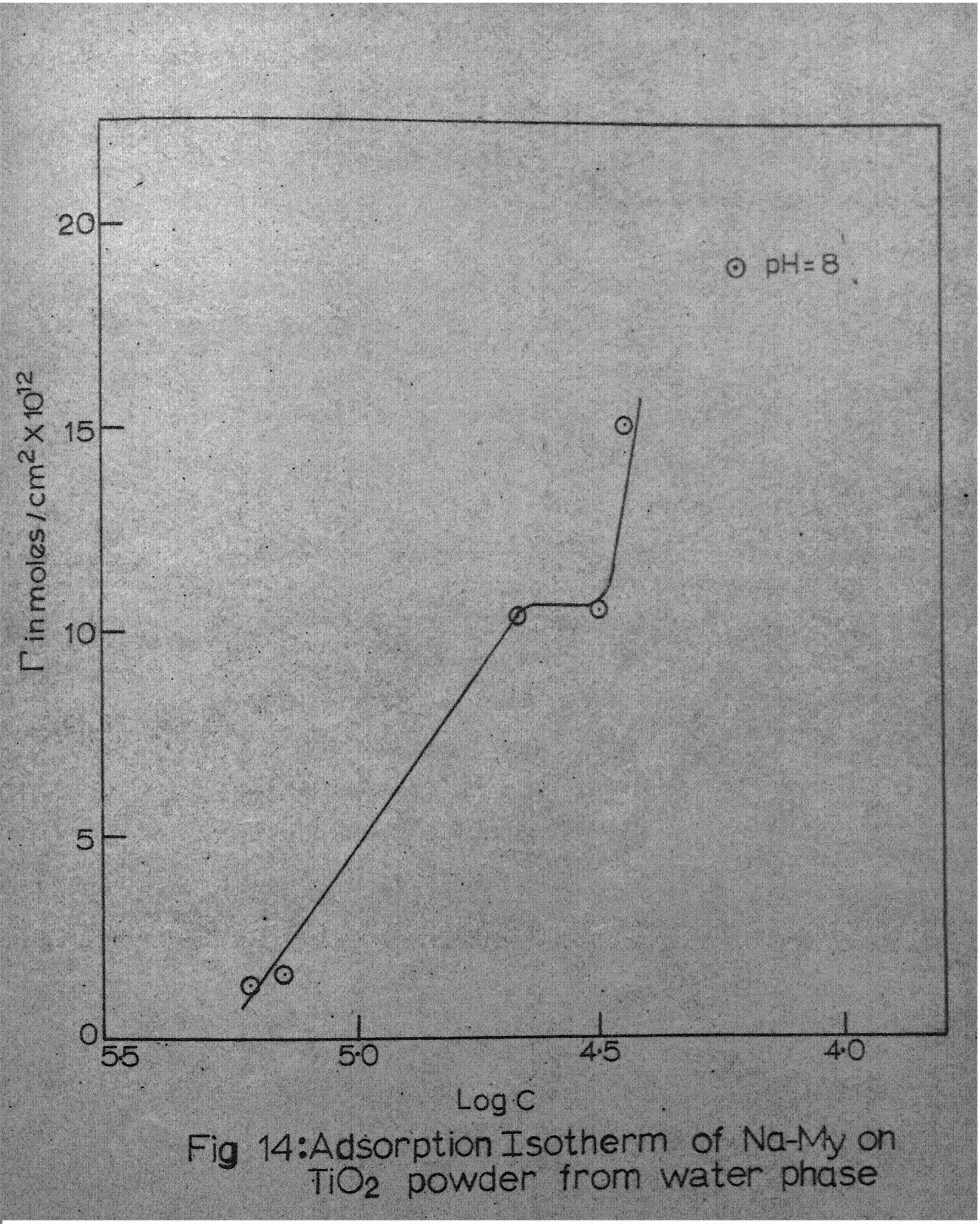

Fig 14: Adsorption Isotherm of Na-My on TiO_2 powder from water phase

equilibriation to take place. Dodecane and aqueous phases were separated using a separating funnel. Two ml. of solution from both dodecane and aqueous phase were transferred to two different planchets and concentrations were measured as described before. The dodecane solution was evaporated at 40°C for a longer time (30 hrs.). The apparent distribution coefficient which has been discussed in Chapter I was calculated. The results have been tabulated in Table 6, and the effect of concentration and pH of the aqueous phase has been shown. Fig. 11 shows the variationof K_D with pH.

3.5 Adsorption Measurement:

Ten ml. of aqueous sodium myristate solution which was equilibrated with dodecane in the previous experiment was taken in a polythene bottle. One gram of the TiO_2 powder is added and the stoppered bottle is shaken vigorously for 30 mins. This was then kept at 30 ± 1°C in a thermostat for six hours. The supernatent liquid is taken out with a pipette and centrifuged at 1500 r.p.m. Two ml. of the clear solution is transferred to the planchet for concentration measurement as before. The amount adsorbed can be calculated from the difference in concentrations.

The results obtained have been tabulated in Table 6, and Figures 12,13 and 14 show the variation of Γ_{SW} (Adsorption density) with concentration and pH.

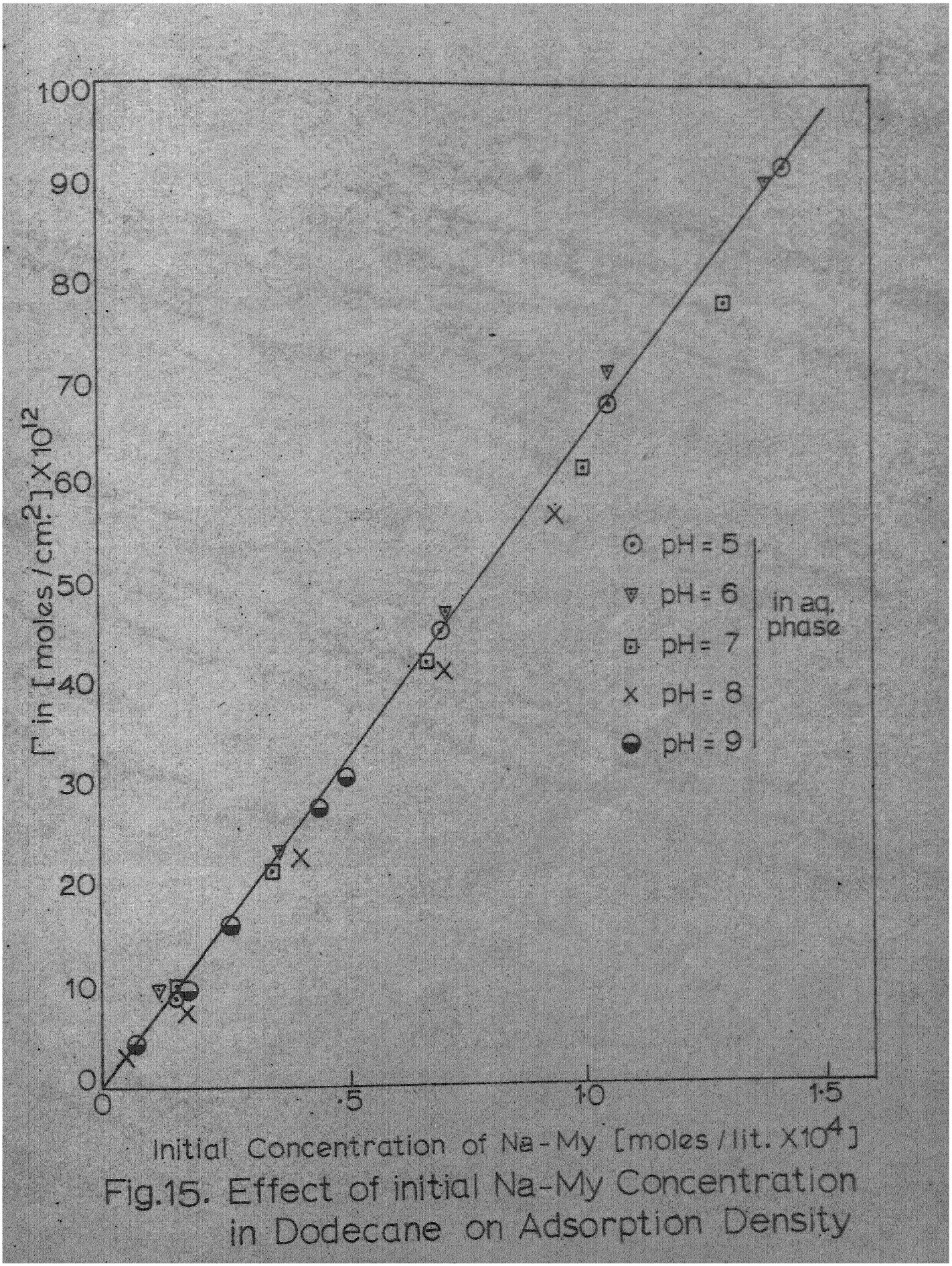

Fig.15. Effect of initial Na-My Concentration in Dodecane on Adsorption Density

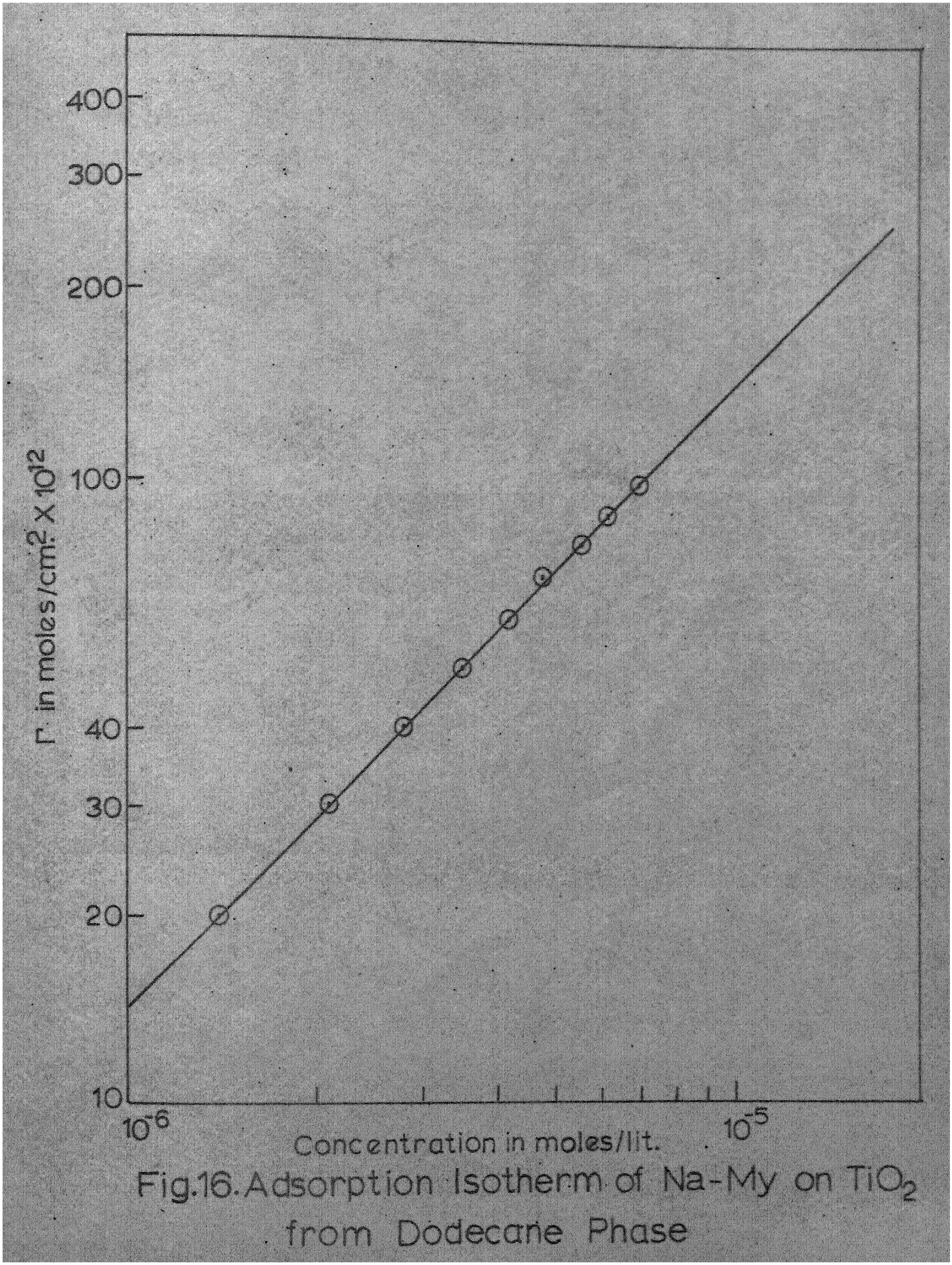

Fig.16. Adsorption Isotherm of Na-My on TiO_2 from Dodecane Phase

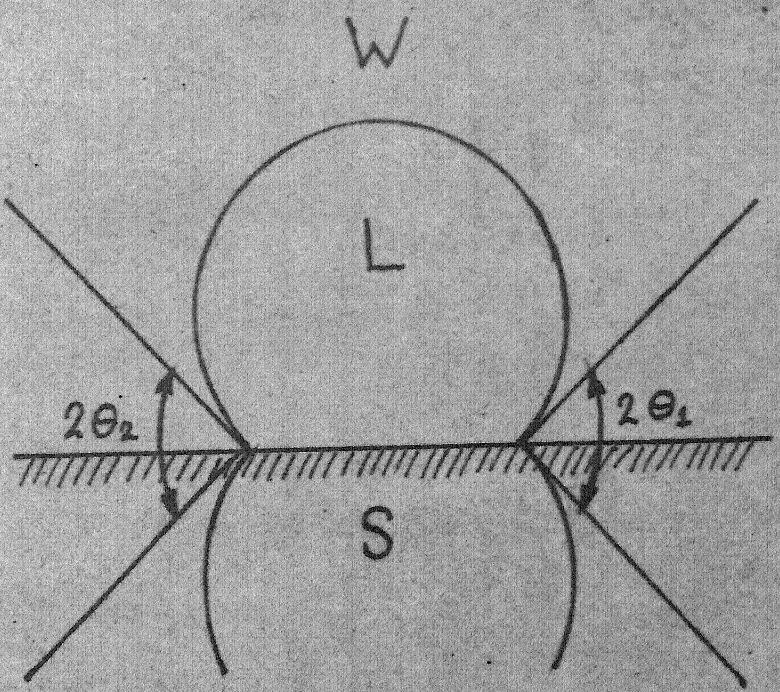

$$\theta_e = \left[\frac{2\theta_1 + 2\theta_2}{2}\right] \times \frac{1}{2}$$

Fig. 8. Measurement of Contact Angle

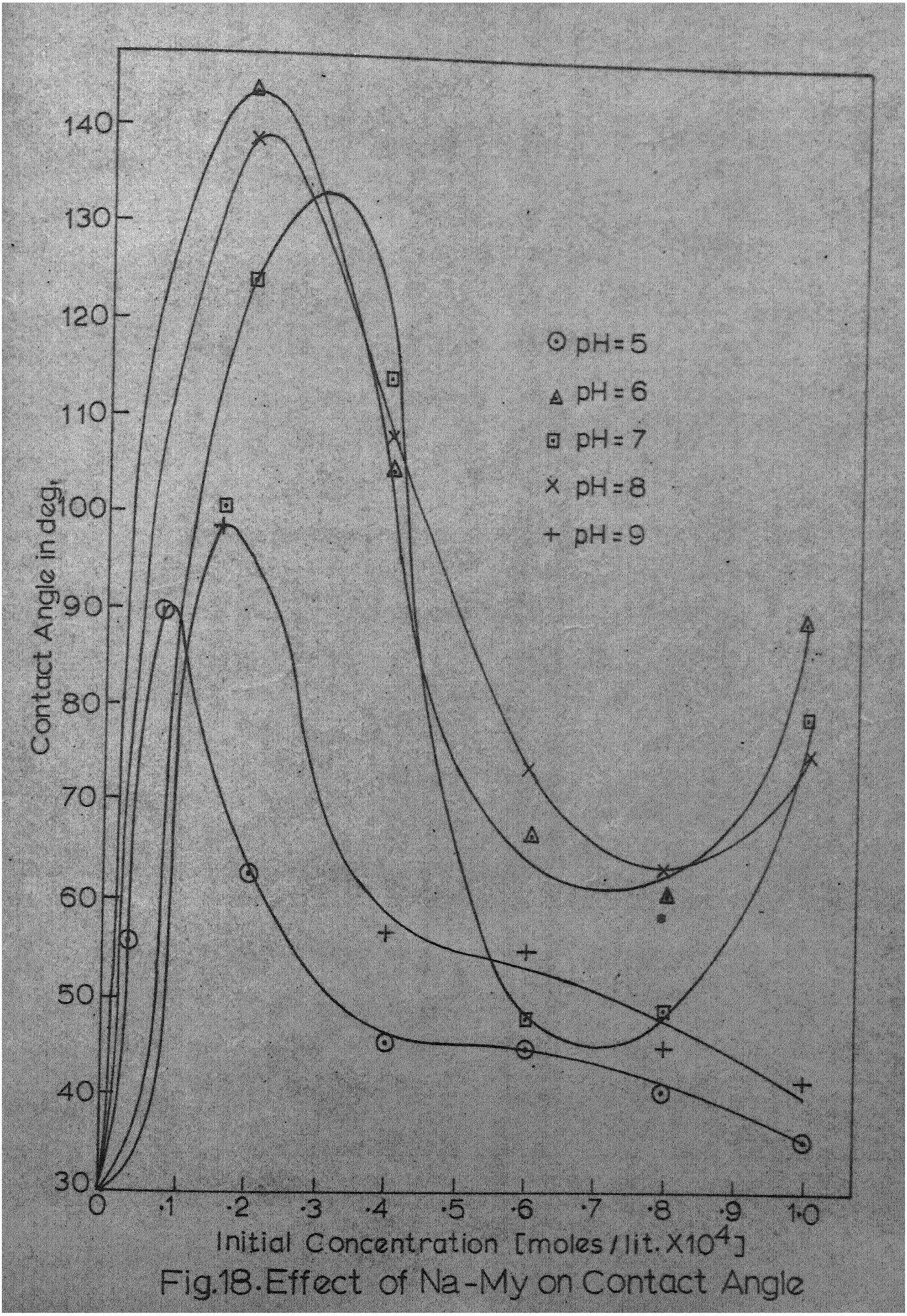

Fig.18. Effect of Na-My on Contact Angle

Similar procedure was adopted for measurement of adsorption from the dodecane phase. The results obtained have been tabulated in Tables 7 and 8 and Fig. 15 shows the variation of adsorption density Γ'_{SL} with initial concentration of Na-My and pH of the aqueous phase. Fig. 16 shows the variation of Γ_{SL} with equilibrium concentration of Na-My.

3.6 Contact Angles:

For the measurement of contact angles captive bubble technique was used. Na-Myristate solution which had been equilibrated with dodecane was taken in a cuvette and the single crystal of rutile was submerged in it. A drop of equilibrium dodecane was then placed on the crystal by a bubble holder. The image of the bubble was projected on a flat paper surface, and the contact angles were measured by drawing tangents at the interface and measuring the angles between the two tangents as shown in Fig. 8.

Contact angles were measured at varying concentrations of Na-My and pH. These have been tabulated in Table 9 and have been plotted against initial concentration of Na-My in Fig. 18.

3.7 Inter-facial Tension at Water/Dodecane Interface:

The interfacial tensions at the water/dodecane interface were measured with the help of Cenco Du-Novy interfacial tentiometer, both the phases were mutually equilibriated by the method discussed earlier.

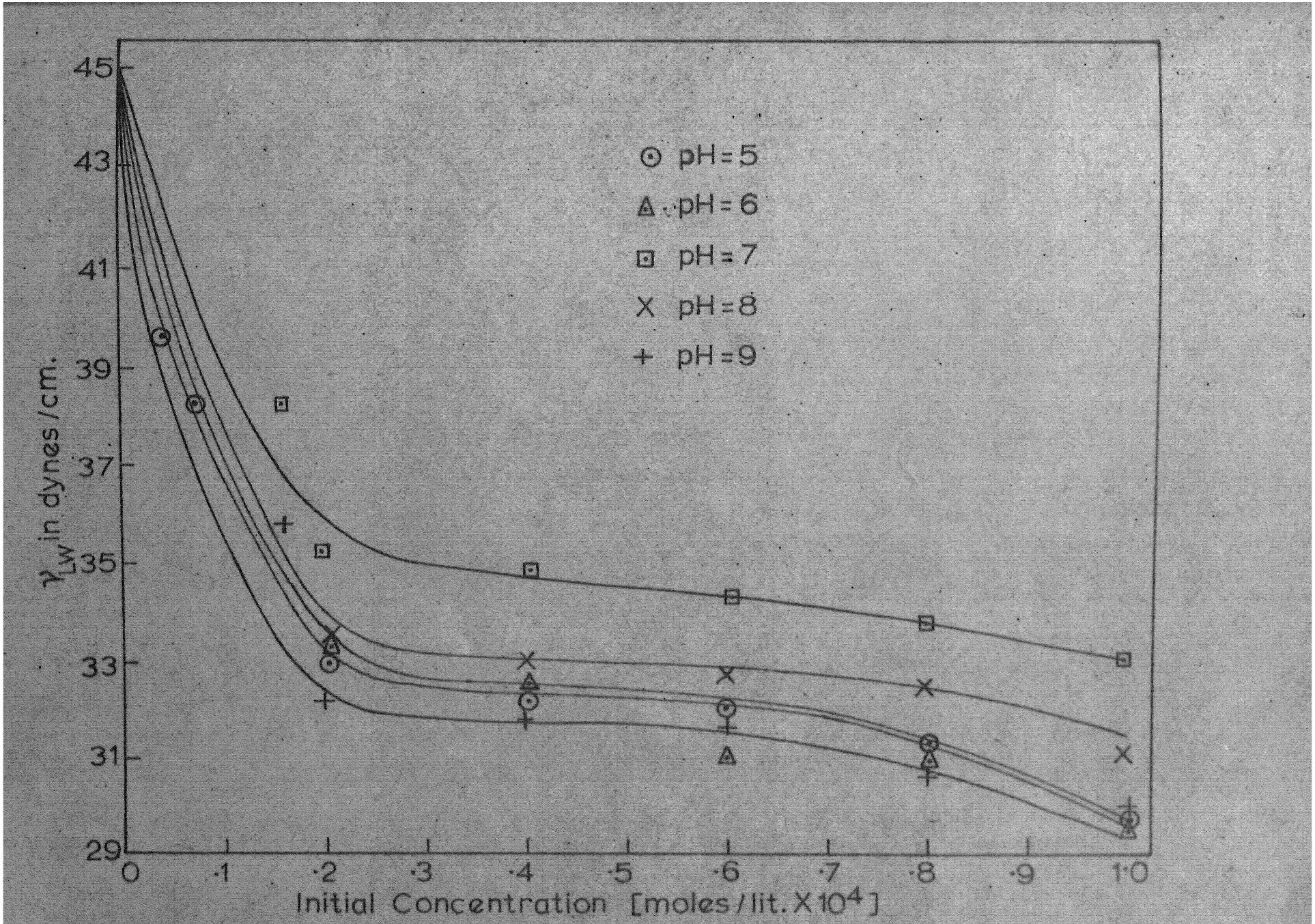

Fig.17. Effect of Na-My on Water-Dodecane Interfacial Tension

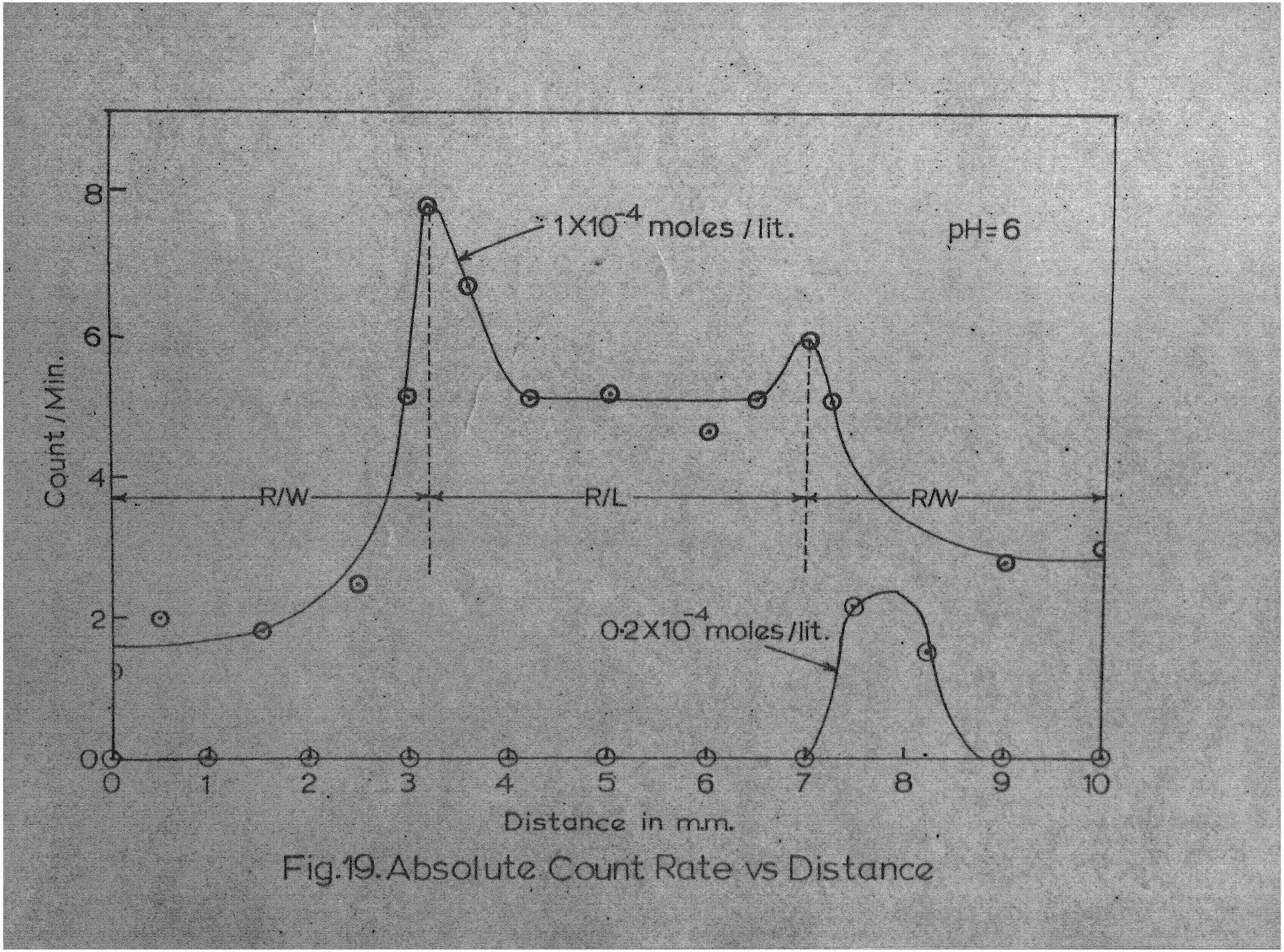

Fig.19. Absolute Count Rate vs Distance

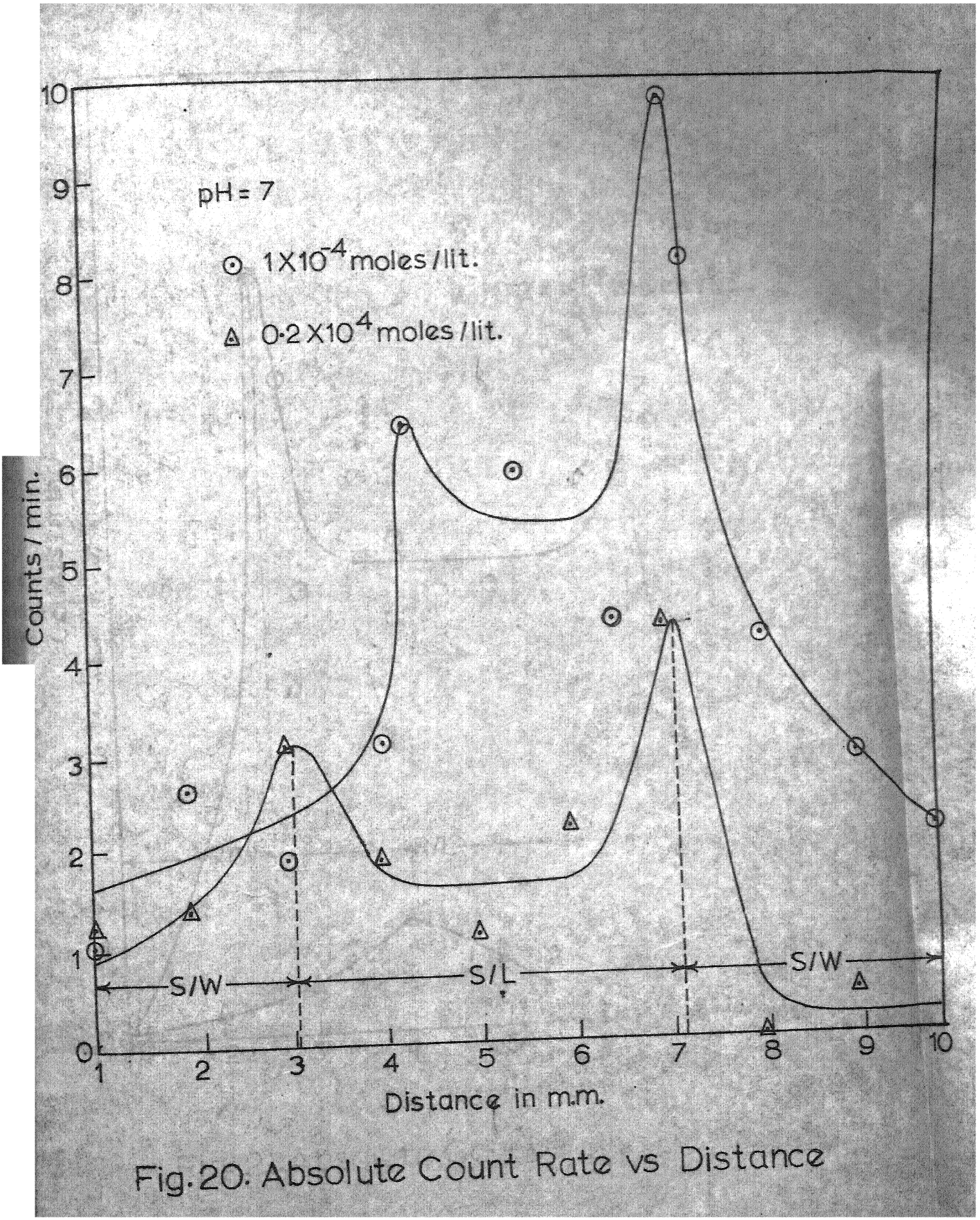

Fig. 20. Absolute Count Rate vs Distance

Interfacial tensions γ_{LW} were measured and have been tabulated in Table 10, and have been plotted against concentration at different pH's in Fig. 17.

3.8 Three-Phase Interline Adsorption Experiment:

Thoroughly cleaned rutile crystal was placed in a cuvette which was filled with equilibriated sodium myristate solution. The dodecane drop was then attached to the surface by a bubble holder, sufficient time (1/2 hr) was allowed for a stable contact to take place. The crystal was then taken out of the cuvette (when the bubble also got detached) and dried in an oven maintained at 40°C.

The crystal was then mounted on the base of a travelling microscope which had a least count of .01 mm.

G.M. counter tube, which had a lead disc. with a fine hold of .004 in. was attached at the bottom, and the whole assembly was mounted on a perspex stand. The entire surface of the crystal was scanned by moving the crystal under the G.M. tube along a diameter.

The absolute count rate at different distances from one end was recorded and has been tabulated in Tables 11 to 13 at different concentrations and pH. Figs. 19 to 21 show the variation in absolute count rate with distance.

CHAPTER IV

COMPUTATION OF CERTAIN PARAMETERS FROM BASIC DATA

To find possible relationships between measured adsorption densities, interfacial tensions and contact angles, certain parameters have been computed.

(1) Distribution coefficient of myristic acid between water and n-dodecane.

(2) Adhesion tension($\gamma_{LW} \cos \theta$)

(3) $\Delta\gamma_{RW}$ from the adsorption isotherm data of aqueous phase.

(4) $\Delta\gamma_{RL}$ from the adsorption isotherm data of dodecane phase.

4.1 Computation of 'D'(Actual Distribution Coefficient):

To calculate the actual distribution coefficient 'D' for myristic acid (RCOOH) where

$$D = \frac{|RCOOH|_o}{|RCOOH|_a} \qquad (4.2)$$

one has to go back to equation (4.1),

$$K_D = \frac{|RCOOH|_o}{|RCOO^-|_a + |RCOOH|_a} \qquad (4.1)$$

substituting (4.2) in (4.1),

$$K_D = \frac{D}{1 + \frac{|RCOO^-|_a}{|RCOOH|_a}} \qquad (4.3)$$

In the aqueous solution of sodium myristate, the following ionic equilibria exists as considered by Dixit and Biswas.[16]

$$RCOO^-_a + Na + H_2O \underset{I}{\overset{K_{h_s}}{\rightleftharpoons}} RCOOH_a + Na^+ + OH^- \qquad (4.4)$$

$$RCOOH_a \underset{II}{\overset{K_F}{\rightleftharpoons}} (RCOO^-_m, RCOOH_m)$$

$$(RCOO^-_m, RCOOH_m) \overset{K_c}{\rightarrow} III$$

$$H^+ + OH^- \rightleftharpoons H_2O \qquad (4.5)$$

$$H^+ + Cl^- \rightleftharpoons HCl \qquad (4.6)$$

$$Na^+ + OH^- \rightleftharpoons NaOH \qquad (4.7)$$

$$RCOOH_s \rightleftharpoons H^+ + RCOO^-_s \qquad (4.8)$$

where $RCOO^-$ represents myristate ions and m stands for micelle and S for solution phase. Two distinct cases have to be realized, one for concentration below c.m.c. and the other above c.m.c.

In the present study the concentration of sodium myristate lies much below c.m.c. which is around 2.9×10^{-4} moles/litre. Hence steps II and III in equation (4-4) do not come into the picture. Thus for the hydrolysis reaction (4.4),

$$\frac{|RCOOH|_a \, |OH^-|}{|RCOO^-|_a} = K_h \qquad (4.9)$$

K_h is the hydrolysis constant. For a mass balance on myristate ions we have,

$$S = (RCOO^-) + (RCOOH) \qquad (4.10)$$

where S is the actual concentration of the sodium myristate added in mole per liter.

Now when S < < c.m.c., the degree of hydrolysis β is the fraction of a gram mole of sodium myristate hydrolyzed at equilibrium is related to K_h by:

$$K_h = \frac{\beta^2 S}{1-\beta} \qquad (4.11)$$

the values of β for several concentrations and temperatures are available (Table 14), for instance at 40°C, β has been reported to be 0.25 for sodium myristate concentrations of 1×10^{-4} moles/litres. K_h was calculated for different values and was found to be $.83 \times 10^{-4}$.

For the hydrolysis reaction (4.8), we define another hydrolysis constant K_a as

$$K_a = \frac{|RCOOH|_a}{|RCOO^-|\ |H^+|} \qquad (4.12)$$

Substituting (4.12) in (4.3)

$$K_D = \frac{D}{1 + \frac{1}{K_a\ |H^+|}}$$

$$= \frac{D.K_a\ |H^+|}{1 + K_a |H^+|} \qquad (4.13)$$

For the reaction (4.5) the hydrolysis constant for water is defined as;

$$K_w = |H^+| \; |OH^-| \qquad (4.14)$$

combining (4.9), (4.12) and (4.14)

$$K_a = \frac{K_h}{K_w} \qquad (4.15)$$

Substituting (4.15) in (4.13)

$$D = \frac{K_D \left| 1 + \left(\frac{K_h}{K_w}\right) (H^+) \right|}{\left| \left(\frac{K_h}{K_w}\right) (H^+) \right|} \qquad (4.16)$$

The actual distribution coefficient D was thus calculated and is tabulated in Table 15.

4.2 Adhesion Tension:

γ_{LW} and cos θ values are obtainable from Tables 9 and 10 and Figs. 17, and 18 for the corresponding concentrations. γ_{LW} cos θ at various concentration and pH have been tabulated in Table 16 and the $\Delta\gamma_{LW}$ cos θ values have also been computed with zero value of θ and myristic acid concentration as the standard point of reference.

4.3 Computation of $\Delta\gamma_{RW}$ from the Adsorption Data:

From Figs. 12, 13 and 14, $\Delta\gamma_{RW}$ values have been computed, by calculating the area under the curve between the two concentration limits.

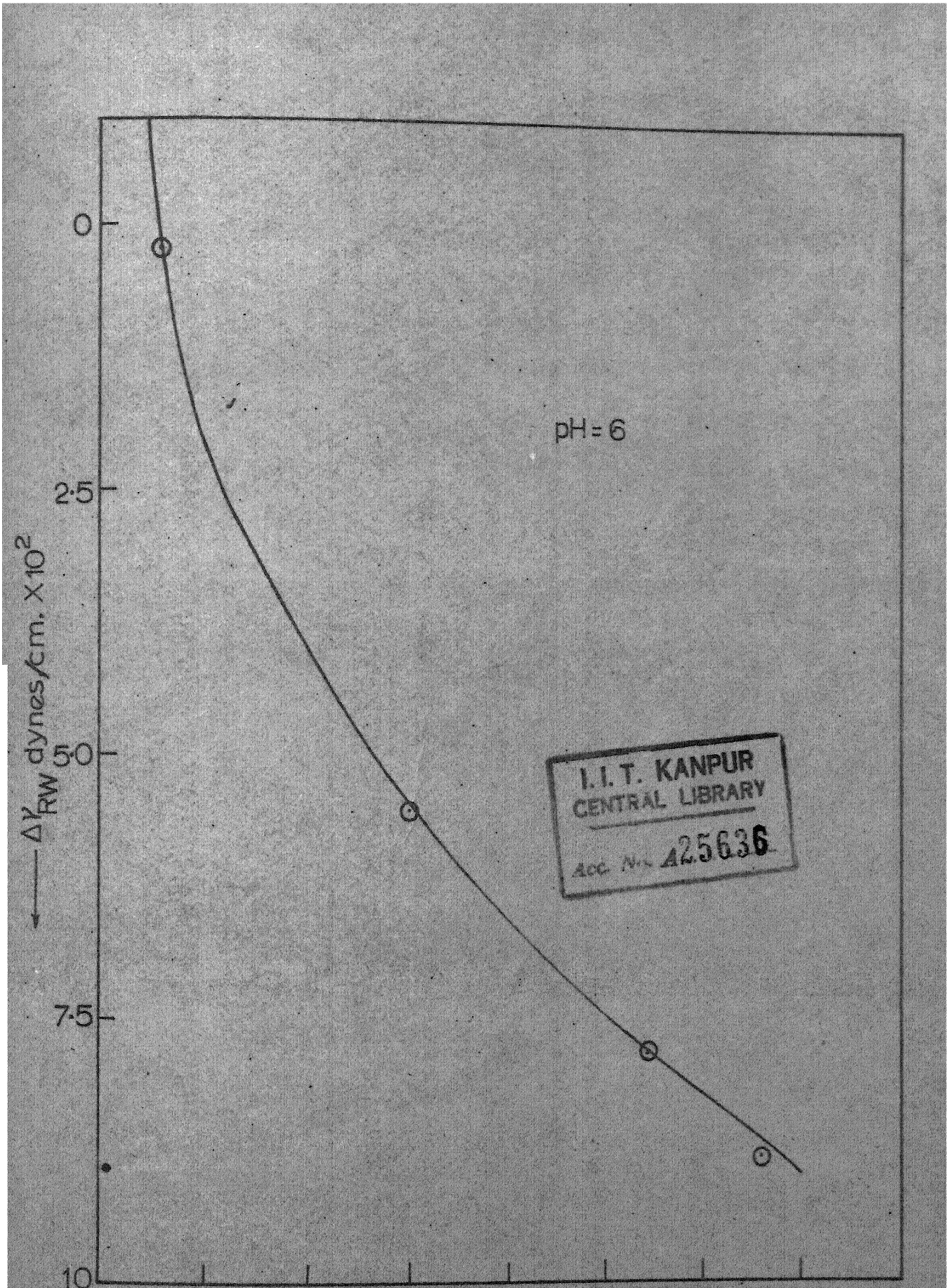

Fig. 22. Variation of $\Delta\gamma_{RW}$ with Na-My Eq. Conc.

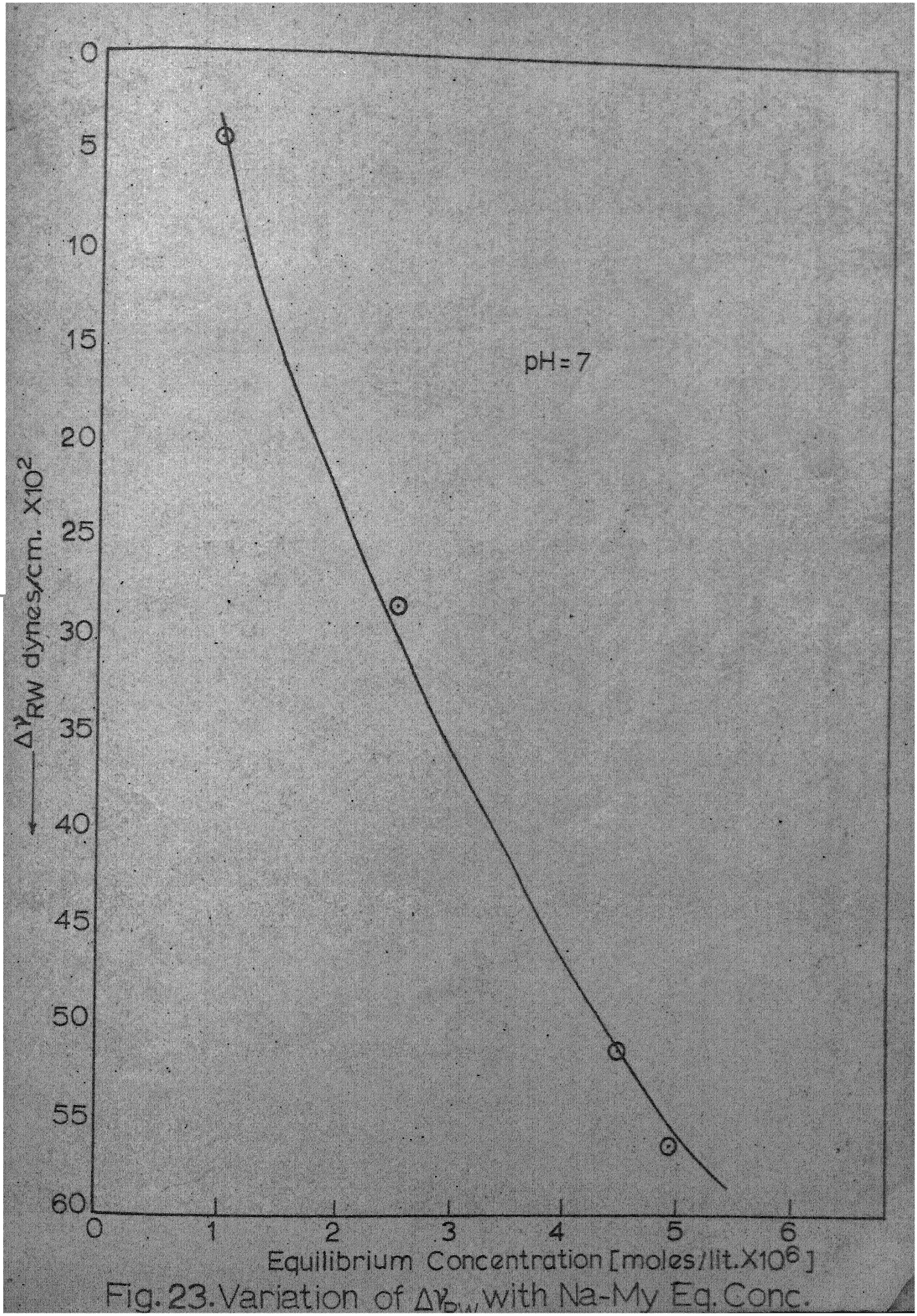

Fig. 23. Variation of $\Delta\gamma_{R/W}$ with Na-My Eq. Conc.

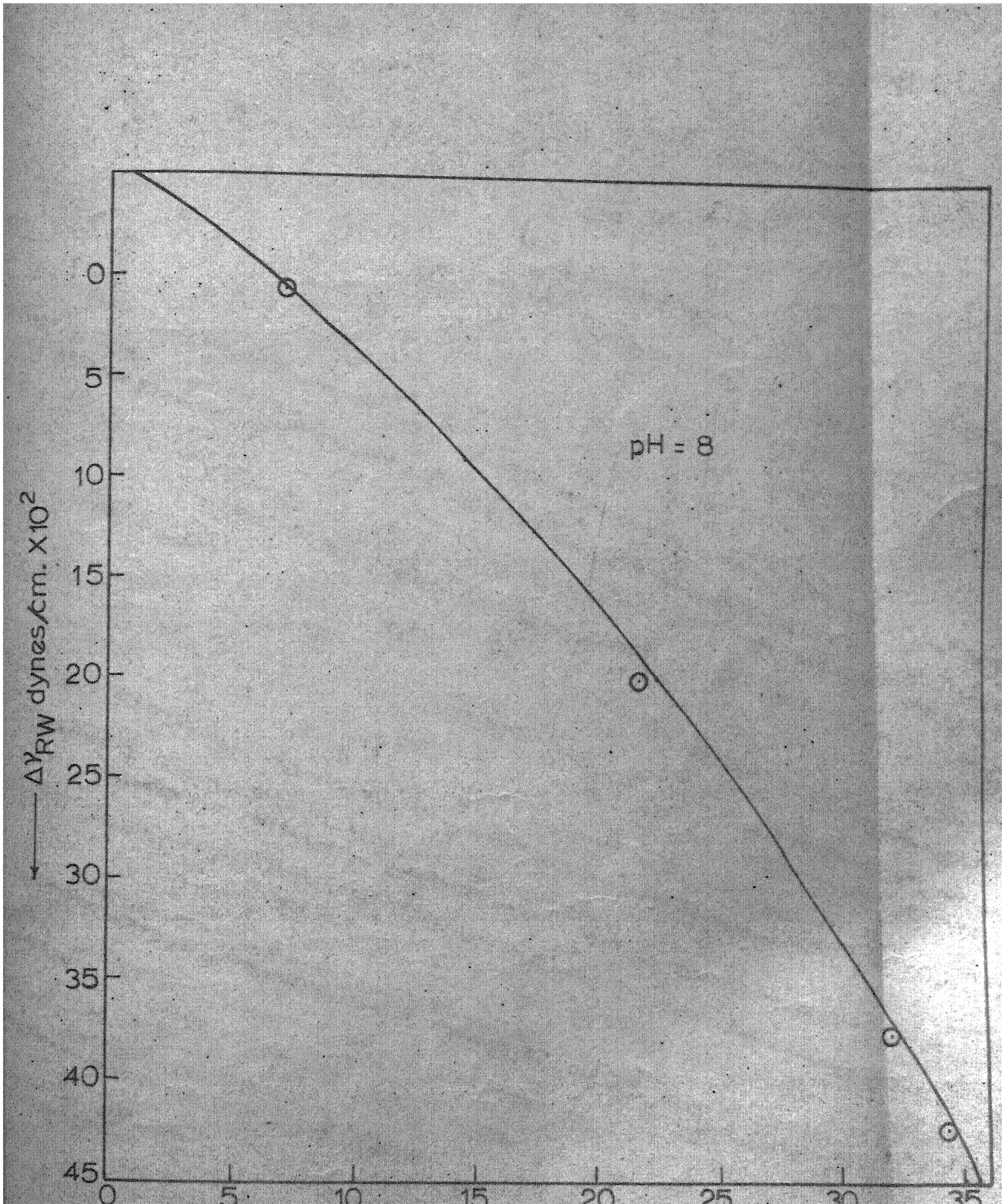

Fig.24. Variation of $\Delta\gamma_{RW}$ with Na-My Eq. Conc.

$$d\gamma_{RW} = -RT\Gamma_{RW}\, d \ln C \qquad (1.8)$$

$$\Delta_{RW} = -RT \int_{C_1}^{C_2} \Gamma_{RW}\, d \ln C \qquad (1.9)$$

$\Delta\gamma_{RW}$ so obtained with zero value of C and Γ as reference points has been plotted against corresponding concentration in Figs. 22 to 24. From zero to the lowest concentration the isotherm is assumed to be linear.

4.4 Computation of $\Delta\gamma_{RL}$ From Adsorption Data:

From Fig. 16, which is a straight line plot between $\log \Gamma_{RL}$ and log C, it can be concluded, the function is of the type.

$$\log \Gamma_{RL} = \log a + b \log C^* \qquad (4.17)$$

The slope of this curve gives b which is calculated to be 1.0015 and the intercept a is calculated to be 1.4×10^{-5}.

Equation (4.17) now reduces to

$$\Gamma_{RL} = 1.4 \times 10^{-5} C^* \qquad (4.18)$$

Now,

$$\Delta\gamma_{RL} = -RT \int_{C_1^*}^{C_2^*} \Gamma_{RL}\, d \ln C^* \qquad (1.10)$$

Substituting (4.18) in (1.10)

$$\Delta\gamma_{RL} = -RT \int_{C_1^*}^{C_2^*} 1.4 \times 10^{-5} \frac{C^*}{C^*} dC^*$$

$$\Delta\gamma_{RL} = - RT \times 1.4 \times 10^{-5} (C_2^* - C_1^*) \qquad (4.19)$$

$\Delta\gamma_{RL}$ values have been computed from equation (4.19).

$\Delta\gamma_{RL}$ and $\Delta\gamma_{RW}$ values so computed are tabulated against their corresponding concentrations and the $\Delta\gamma^{**}$ values are compared with $\Delta\gamma_{WL}$ cos θ values in the same concentration range in Table 17.

** = | RL − RW |.

CHAPTER V

DISCUSSIONS

5.1 Distribution Coefficient:

With the increase in pH (Fig. 11) K_D decreases. This is because of the fact that as pH increases the degree of dissociation increases giving greater percentage of myristate ion which is more compatible in the aqueous phase. Myristic acid on the other hand is formed at lower pH and is more soluble in dodecane phase. It was expected from the theoretical treatment given in (4.1) the previous chapter that K_D-pH relationship should be linear with a slope of -1[12] and thus would correspond to some constant value of D (distribution coefficient of myristic acid between dodecane and water phase).

Fig. 11 shows that K_D-pH relationship is linear but the slope is much greater than unity (1.8). The magnitude of D is not very large and shows a decrease with increasing pH. Thus, the physico-chemical system is not as simple as postulated in the previous pages and outlined by Shergold and Mellgren[12] in a similar system. It is plausible that solubility of myristic acid in the water phase is augmented considerably in presence of OH^- and myristate ion. Hence the pH dependence of the distribution coefficient.

5.2 Adsorption Experiments:

(a) From Aqueous Phase:

Maximum adsorption seems to be taking place at pH = 7, and the adsorption density is nearly zero at pH = 5 (Table 6 and 9). The extent of coverage is 5 percent of the monolayer, the thickness of which comes out to be 6.6×10^{-10} moles/li when the cross sectional area of the myristate molecule is taken to be 25 $Å^2$.[34] Explanation for such a kind of behaviour is to be sought in the prevailing ionic conditions in the aqueous bulk phase and the effects of different ionic species, e.g. H^+ and OH^- etc. on adsorption.

Qualitatively the action of H^+ and OH^- ions on the collector adsorption can be divided into the following[25]

(1) The concentration of hydrogen ions affect the degree of dissociation of collector molecules into ions

(2) H^+ and OH^- ions get adsorbed either in the internal or external part of the double layer changing the electrochemical and electrokinetic potential and thus affect the collector adsorption on to the surface or on the double layer.

(3) Hydroxyl ions can compete with collector anions and hydrogen ions with cations or neutral molecules during their adsorption on the surface.

(4) They can remove or favour adsorption of other ions which are detrimental to the adsorption of the collector.

This explains almost zero Adsorption at pH = 5 and 9 because at pH = 5 there is an abundance of H^+ ions and at pH = 9, that is an abundance of OH^- ions. At pH = 9, OH^- behaves as a competitor to the myristate ion being adsorbed and at pH 5 there is more of undissociated fatty acid which is probably not as strongly adsorbed from the aqueous phase as the fatty anion.

(b) Adsorption From Dodecane Phase:

There is hardly any effect of aqueous solution pH on the adsorption from dodecane phase, and therefore irrespective of pH a straight line was obtained when Γ_{RL} was plotted against the initial concentration barring some minor scatter (Table 7). This strongly suggested that there should be one and only one adsorption isotherm for Na-My on rutile irrespective of pH in the aqueous phase, since identical proportions of material were used for all experiments pertaining to adsorption from the organic phase. The adsorption isotherm in the organic phase as computed from the Fig. 15 also turns out to be linear (Fig. 16). The extent of coverage is 15 percent of the monolayer (Table 9).

5.3 Interfacial Tension:

Interfacial tensions of dodecane-water interface decreased considerably upto aqueous concentrations of 0.2×10^{-4} moles/lit, beyond this concentration of $.2 \times 10^{-4}$ moles/lit the decrease in interfacial tension is gradual.

5.4 Contact Angles:

The contact angle is plotted against concentration and pH in Fig. 18, upto a concentration of .2 x 10^{-4} moles/lit, it increases, beyond which they start decreasing and in case of pH = 6,7,8 they shoot up again beyond .7 x 10^{-4} moles/lit. initial concentration of Na-Myristate.

These plots are somewhat unconventional. Usually contact angles increase from zero (clean surface) to around 90° or beyond systematically, with increase of collector concentration. In the present system, special care was taken to clean the single crystal surface every time before use.

The procedure for cleaning the surface was the same as adopted by Gaudin, Biswas, Witt[31]. The rutile crystal was cleaned with hot chromic acid followed by distilled water, concentrated hydrochloric acid, and again distilled water and conductivity water, and it was checked before the contact angle experiment, that the dodecane drop makes no contact with the rutile crystal placed in conductivity water.

Adsorbtion of H^+, OH^-, dodecane etc. apart from collector may be responsible for the unprecedented nature of the curves which cannot be thoroughly explained.

5.5 Adsorption Magnitude at the 3-Phase Inter-Line:

An attempt was made to determine the exact amount adsorbed at the three-phase inter-line using the C_{14} tracer. A series of apertures ranging from .01 mm to 1 mm were employed, and the quantity of labelled material was increased 60 fold to get an appreciable count rate which is outside the limit of errors. Inspite of the constant efforts put in, it was seen that no matter how much one increases the diameter of the hole in the lead disc. and no matter how much of labelled material is there, the count rate came out to be very very low. The reasons for this kind of behaviour probably is the low activity of the radioactive source high self-scattering and self-absorption ratios. The crystal surface was scanned and it was inferred that the count rate gives the relative amount of material adsorbed at different interfaces and the three-phase inter-line (Tables 11,12 and 13, Figs. 19, 20 and 21).

5.6 Correlation of Contact Angle Interfacial Tension and Adsorption Density:

The equilibrium contact angle cannot be computed, as there is no means of evaluating γ_{RL} and γ_{RW}. However, changes in the product $\gamma_{LW} \cos\theta$ with increasing myristate can be computed and compared to the experimental data.

This has been accomplished with the aid of Gibbs adsorption equation which relates changes of interfacial

tension to surfactant adsorption density and concentration. From the equilibrium myristate adsorption density - concentration curves given in Figs. 12, 13, 14 and 16 were integrated to gives changes in the rutile-dodecane and rutile-water interfacial tensions as a function of myristate concentration at constant pH and ionic strength.

The rutile water interfacial tension did not change significantly. The γ_{RL} values decreased rapidly as a function of the sodium myristate collector.

The assumption here is that the adsorption of water and dodecane do not alter the interfacial tensions of rutile-dodecane and rutile water at a constant pH and varying collector concentration.

As myristate concentration in increased at constant pH, the Young's equation relates the change of γ_{RL} and γ_{RW} to the changes of the product $\gamma_{LW} \cos \theta$.

In Table 17, the change in $\Delta\gamma_{RL}$ and $\Delta\gamma_{RW}$ obtained from adsorption measurements are compared to values of $\gamma_{LW} \cos \theta$ obtained experimentally. Although the values are not same the orders of magnitudes are the same. This may be due to erroneous computations of $\Delta\gamma_{SL}$ and $\Delta\gamma_{SW}$ terms. Adsorption of dodecane, water H^+, OH^- on solid surface has not been taken into account and this may play some role in changing the interfacial tension values. Besides Gibbs adsorbtion equation may not be fully applicable if the natureof adsorption is chemisorption type, as has been pointed out by Mazumdar and

Vishwanathan[19] for Na-Oleate-rutile system, using I.R. technique. But Bansal[26] has not been able to get any peak, in the IR analysis so the subject is still controversial.

Further more, excessive adsorption at the interline clearly shown in this system, Fig. 19,20 and 21 and also observed by Majumdar and Viswanathan[19] seems to have been ignored in the theoretical treatment and hence one may conclude that the application of Young's equation and Gibbs adsorbtion equation is difficult.

The difference in $\Delta\gamma_{SL} - \Delta\gamma_{SW}$ is very small, therefore can be said that $\Delta\gamma_{LG} \cos\theta$ is of same magnitude as $\Delta\gamma_{SL}$ since $\Delta\gamma_{SW}$ is negligible. The above observation coupled with the verification of a previous postulate that $\Gamma_{SL} > \Gamma_{SW}$ (Table 16) points to the conclusion that adsorbtion at solid liquid interface is much more crucial than at the solid water interface. Decker and Gaudin obtained a similar conclusion. It is surprising that Shergold and Mellgren[11] who worked on hematite iso-octane-water system did not measure Γ at solid liquid interface.

5.7 Conclusions and Predictions on Recovery of Slimes at the Liquid Water Interface:

It may be pointed out that Shergold and Mellgren[8,11,12,13] achieved success in recovery of ultra fine particles. They explained the dependence of such a process on surfactant-

concentration and pH and pointed out[8] how an unique value of optimum pH was obtained (6-8).

In the present series also, fundamental studies point towards the feasibility of a technological process of recovery of rutile slime in water-dodecane interface with sodium myristate as collector. It may be predicted that optimum collector concentration should be in the range of .4 to about.8 x 10^{-4} moles/lit. and pH around 7, (Figure 25). Further work is contemplated to verify the predictions.

The present series of work indicates that three phase contact angle and adhesion tension clearly depend on the adsorption magnitude and interfacial tensions in the three interfaces which in their turn have concentration and pH dependence. The relationship between the above parameters and actual interfacial concentration of slimes should be the subject matter of subsequent investigations.

REFERENCES

1. A.M. Gaudin, 'Flotation' (New York: McGraw Hill Book Co. Inc. 1932 p. 161).

2. A.K. Biswas, 'Met. E. 604- Surface Phenomenon in Chemistry and Metallurgy', Class Notes.

3. P.L. De Bruyn and G.E. Agar, 'Surface Chemistry of Flotation', 50th Anniversary Flotation Volume, AIME, 1962, 91-138.

4. P.L. De Bruyn, J.Th. G. Overbeek, R. Schuhmann, 'Flotation and the Gibbs Adsorption Equation', S.M.E., AIME, 1954, 6, 519.

5. Smolden, Rec. Trav. Chim, 80, 1961.

6. J.H. Schulman and J. Leja, 'Control of Contact Angles at the Oil-Water-Solid Interfaces', Trans. Faraday Soc., 50, 1954, 598-605.

7. F.F. Aplan and P.L. De Bruyn, 'Adsorption of Hexyl Mercaptan on Gold,' SME, AIME, 1963, 226, 235.

8. O. Mellgram and H.L. Shergold, 'Method for Recovering Ultrafine Mineral Particles by Extraction with an Organic Phase', Trans. IMM London, 1966, 75, C 267-8.

9. T. Decker and A.M. Gaudin, 'Contact Angles and Adsorption in the System Quartz-water Dodecane Modified by DAC', Journal Coll. and Interface Science, 24, 1967, pp. 151-158.

10. P. Somasundaram, 'The Relationship Between Adsorption at Different Interfaces and Flotation Behaviour', SME AIME March, 1968, 105-108.

11. H.L. Shergold and O. Mellgren, 'Concentration of Minerals at the Oil-Water System in the Presence of Sodium Dodecyl Sulphate', Trans. IMM, 78, C 121-32, 1969.

12. H.L. Shergold and O. Mellgren, 'Concentration of Minerals at the Oil/Water Interface,' SME, AIME, 247, 149-159, 1970.

13. H.L. Shergold and O. Mellgren, 'Concentration of Hematite at the Iso-octane Water Interface with Dodecyl Amine as Collector', Trans. IMM 80, C 60 - C 68, 1971.

14. I.J. Lin and A. Metzer, 'Adsorption Densities on Interfaces in Three Phase System', J. Coll and Interface Science, 40, No. 2, 1972.

15. J. Powney and D.O. Jordon, 'The Hydrolysis of Soaps as Determined from Glass Electrode and pH Measurements', Trans. Fara. Soc. 34, 1938, p. 363.

16. S.C. Dixit, A.K. Biswas, 'pH-Dependence of the Flotation and Adsorption Properties of Some Beach Sand Minerals', SME, AIME, 244, 1969, 173-178.

17. I.N. Plaskin, 'Using Microautoradiography for the Study of the Interaction Reagents with Minerals in Flotation', 2nd International Congress, of Surface Activity, Vol. 3, 1957, 355-360.

18. I.N. Plaskin and R. Sh. Shafeyer, 'On Properties of Distribution of Xanthate on the Surface of Sulphide Minerals', Journal of Mines, Metals and Fuels, July 1960.

19. Mazumdar and Vishwanathan, 'Collector Regulator Interactions in the Flotation of Beach Sand Minerals Under Conditions of Soap Flotation', Trans. IIM 26, No. 1, Feb. 1973.

20. A.F. Taggart, 'Handbook of Mineral Dressing', John Wiley and Sons, Inc., New York, 1945.

21. G.L. Sinard, M. Burke, D.J. Salley, SME, Trans. AIME 187, 1950, p. 359.

22. A.M. Gaudin and F.W. Bloecher, SME, Trans. AIME, 187, 1950, 499.

23. A.M. Gaudin and P.L. De Bruyn, 'Radioactive Tracess in Mineral Engineering Problems Particularly in Flotation', Canadian Min. Metall. Bull. 42, 1949,331.

24. A.M. Gaudin and C.S. Chang, SME, AIME, 193, 1952,193.

25. S.G. Dixit, Ph.D. Thesis, IIT Kanpur.

26. V.K. Bansal, M. Tech. Thesis, IIT Kanpur.

27. M.L. Corrin and W.D. Harkin, 'Determination of the Critical Concentration for Micelle Formation in Solutions of Colloidal Electrolytes by the Spectral Change of a dye', J. Am. Chem. Soc. 69, 1947, 679.

28. A.K. Biswas, B.K. Mukherji, 'A Study on Micellar Growth in Surfactant Solutions', J. of Phys. Chem. 64, 1960, p. 1.

29. J. Powney and C.C. Addison, 'The Surface Activity and Critical Concentrations of Aqueous Solutions of Saturated Soaps under Conditions of Suppressed Hydrolysis', Trans. Farad. Soc. 34, 1938, 372.

30. C.H. Giles, and S.N. Nakhwa, 'Studies in Adsorption XVI, The Measurement of Specific Surface Areas of Finely Divided Solids by Solution Adsorption', Journal Appl. Chem., 12, 1962, 226.

31. A.M. Gaudin, A.F. Witt, A.K. Biswas, 'Hysteresis of Contact Angles in the System Organic Liquid-Water-Rutile, SME, AIME, March, 1964, p. 1.

32. S.S. Kajiji and D.M. Desai, 'Properties of K-Oleate', Science and Culture India, 12, 1962, 226.

33. A.C. Zettlemoyer, J.J. Cherrih and C.M. Hollabaugh, 'Estimation of the Surface Polarity of Solids from Heat of Wetting Measurements',J. Phys. Chem. 62, 1958, 489.

34. Schneider, V.L., et.al., 'A Monolayer Study of the Isomerism of Unsaturated and Oxy Fatty Acids', J. Phys. and Coll. Chem. 53, 1949, p. 1016.

Table 1

Properties of Myristic Acid

$CH_3(CH_2)_{12}\ CO_2H$

Mol. Wt. :	228.36
Specific Gravity:	.853
Melting point:	57 - 58°C
Boiling point:	250.5°C
Water solubility:	Nil (1 gm./ 100 ml. of water)

Table 2

Properties of n-Dodecane

$CH_3(CH_2)_{10}\ CH_3$

Mol. Wt. :	170.33
Refractive Index:	1.421
Specific Gravity:	0.751
Melting point:	-9.6°C
Boiling point:	215°C
Water solubility:	Nil

Table 3

Effect of Na-My on Specific Conductance

Sl.No.	Concentration moles/lit.x10^4	Specific conductivity K x 10^2
1	6.25	5.36
2	4.35	3.92
3	3.22	3.12
4	2.44	2.56
5	2.17	2.48
6	2.00	2.42
7	1.74	2.32
8	1.43	2.16
9	1.25	2.08
10	1.12	1.92

Table 4

Variation of Absorbance with Na My Concentration

Sl.No.	Concentration moles / lit x 10^4	Absorbance
1	.8	.27
2.	1.0	.34
3	2.0	.35
4	3.0	.43
5	4.0	.48
6	5.0	.46

Table 5

Determination of Adsorption Isotherm for the System TiO_2/PNP

Sl. No.	Absorbance values after equilibriation with PNP at 400 m .	Corresponding concentrations from standard curve moles/lit $x10^5$	Corrected concentrations after adjusting dilutions	Initial concentrations of PNP	Number of moles transferred per gm. of PNP.
1.	.39	6.0	6×10^{-3}	7.2×10^{-3}	24.0
2.	.22	3.41	3.41×10^{-3}	5.0×10^{-3}	21.8
3.	.325	5.0	$5x5 \times 10^{-4}$	1.0×10^{-3}	10.0
4.	.14	2.2	2.2×10^{-4}	7.2×10^{-4}	10.4
5.	.10	1.6	1.6×10^{-4}	3.6×10^{-4}	4.0
6.	.24	3.75	3.75×10^{-5}	5.76×10^{-5}	.4

Table 6: Adsorption from Aqueous Solution on TiO_2 Powder.

Sl. No.	pH	Initial amount/ 2 ml (moles) x10^{8}	Initial concn. moles/ lit. x10^{5}	Count rate/min. after equilib-riation solid	Corres-ponding amount in moles x10^{8}	Amount adsor-bed in moles/ gm. x10^{8}	Amount adsorbed in moles/ cm^{2} x10^{12}	Equili-brium concn moles/ lit. x10^{5}
1.	5	1.0	0.5	63	1.0	0	0	0.5
2.		1.0	0.5	66	1.0	0	0	0.5
3.		0.7	0.35	56	0.8	0	0	0.35
4.		0.3	0.15	25	0.35	0	0	0.15
5.		0.15	0.075	16	0.20	0	0	0.075
1.	6	1.9	0.95	88	1.32	0.58	1.0	0.66
2.		1.25	0.625	77	1.10	0.15	4.0	0.55
3.		1.0	0.50	40	0.60	0.40	1.30	0.3
4.		0.5	0.25	8	0.12	0.38	1.25	0.06
5.		0.2	0.1	6	0.09	0.11	.35	0.045
1.	7	3.0	1.5	66	0.99	10.05	32.0	0.49
2.		2.0	1.0	60	0.90	5.5	17.9	0.45
3.		1.45	0.725	34	0.51	4.7	15.3	0.255
4.		0.10	0.05	4	0.06	0.20	4.65	0.03
5.		0.5	0.25	13	0.195	1.515	.65	0.098
1.	8	7.8	3.9	490	6.86	4.7	15.3	3.43
2.		7.1	3.55	459	6.43	3.35	10.9	3.215
3.		5.	2.50	310	4.34	3.30	10.75	2.17
4.		3.0	1.50	101	1.414	7.93	25.9	0.707
5.		1.4	0.7	88	1.22	0.90	2.95	0.61
1.	9	13.5	6.75	971	13.5	0	0	6.75
2.		11.5	5.75	833	11.5	0	0	5.75
3.		4.2	2.10	293	4.2	0	0	2.1
4.		3.0	1.5	228	3.0	0	0	1.5
5.		1.3	0.65	80	1.3	0	0	0.65

Table 7: Adsorption From Organic Phase (Dodecane).

Sl. No.	pH	Initial amount in two ml. |moles| x10^8	Initial concn. moles/ lit. x10^4	Count rate (/Min.) after eqbln. with solid	Corres-ponding amount in moles x10^8	Amount adsor-bed in moles/ gm x10^8	Amount adsor-bed in moles/ cm^2 x10^{12}	Eqbln. concn. in moles/ lit. x10^5
1.	5	28.5	1.465	24	0.35	28.15	91.65	0.175
2.		21.0	1.05	17	0.19	20.81	68.0	0.095
3.		13.95	0.70	11	0.12	13.83	45.15	0.06
4.		7.05	0.36	7	0.09	6.96	22.65	0.045
5.		2.925	0.15	6	0.08	2.845	9.30	0.04
1.	6	28.0	1.4	14	0.1	27.9	91.	0.05
2.		21.2	1.06	6	0.09	21.91	71.50	0.045
3.		14.0	0.7	5	0.08	13.92	45.50	0.04
4.		7.0	0.35	4	0.05	6.95	22.65	0.025
5.		2.8	0.14	2	0.03	2.77	9.05	0.015
1.	7	26.0	1.3	130	1.9	24.1	78.5	0.95
2.		20.0	1.0	77	1.1	18.9	61.5	0.55
3.		13.4	0.67	27	0.4	13.0	42.35	0.2
4.		6.8	0.34	16	0.24	6.56	21.40	0.12
5.		2.92	0.15	9	0.12	2.80	9.15	0.06
1.	8	18.8	0.94	106	1.5	17.3	56.50	0.75
2.		13.8	0.69	73	1.0	12.8	41.75	0.50
3.		7.8	0.39	69	0.98	6.9	22.50	0.49
4.		3.08	0.154	29	0.4	2.68	8.75	0.20
5.		0.92	0.46	16	0.1	0.82	2.70	0.05
1.	9	10.00	0.5	30	0.3	9.7	31.65	0.15
2.		8.80	0.44	16	0.16	8.64	28.15	0.08
3.		5.20	0.26	16	0.15	5.05	16.40	0.075
4.		3.08	0.154	12	0.12	2.96	9.70	0.06
5.		1.20	0.06	9	0.10	1.10	3.59	0.05

Table 8

Adsorption from Dodecane Phase on TiO_2 powder

Sl. No.	moles/cm^2 x 10^{12} |A|	Amount absorbed |A| x 1.53 x 10^4	Initial concentration x 10^4	Initial amount in moles x 10^7	Final amount in moles x 10^7	Equilibrium concentration x 10^6
1.	10	1.53	.16	1.6	.07	.7
2.	20	3.06	.32	3.2	.14	1.4
3.	30	4.59	.48	4.8	.21	2.1
4.	40	6.12	.64	6.4	.28	2.8
5.	50	11.65	.80	8.0	.35	3.5
6.	60	9.18	.96	9.6	.42	4.2
7.	70	10.71	1.12	11.2	.49	4.9
8.	80	12.24	1.28	12.8	.56	5.6
9.	90	13.77	1.44	14.4	.63	6.3
10.	100	15.30	1.50	15.0	.70	7.0

Table 9

Effect of pH on Contact Angles in the System Rutile Water-Dodecane, Varying the Concentration of Sodium Myristate in Water.

S.No.	Concn. of Na My in water moles/lit.	Contact Angles				
		pH = 5	6	7	8	9
a	0^o	0^o	0^o	0^o	0^o	0^o
1.	$.04 \times 10^{-4}$	55.8	-	-	-	-
2.	$.08 \times 10^{-4}$	90.0	-	-	-	-
3.	-	-	-	-	-	-
4.	$.16 \times 10^{-4}$	-	-	100.3	-	99.75
5.	$.2 \times 10^{-4}$	63.0	144.5	124.1	138.8	63.75
6.	$.4 \times 10^{-4}$	45.6	105.4	114.6	108.0	57.25
7.	$.4 \times 10^{-4}$	45.0	67.8	48.0	74.1	55.0
8.	$.8 \times 10^{-4}$	40.4	61.4	49.0	62.1	45.1
9.	1×10^{-4}	35.6	90	79.2	76	42.1

Table 10

Effect of pH on Interfacial Tension of Water/Dodecane Varying the Concentration of Na-Myristate

Sl.No.	Concn. of Na-My (Initial) moles/lit x 10^4	Interfacial tension in dynes/cm				
		pH = 5	6	7	8	9
1	0	45	45	45	45	45
2	.04	39.7	-	-	-	-
3	.08	38.3	-	-	-	-
4	.16	-	-	38.3	-	35.8
5	.20	32	33.1	35.2	33.5	32.1
6	.40	32.3	32.5	34.8	33.0	31.7
7	.60	32.1	31.0	34.2	32.7	31.6
8	.80	31.3	31.0	33.7	32.5	30.7
9	1.0	29.7	29.6	33.0	31.0	30.0

Table 11

Variation of Absolute Count Rate with Distance

pH = 6 Concentration = $.2 \times 10^{-4}$ moles/lit.

Sl.No.	Distance	Counts/10 minutes	Zero/10 minutes	Count/minute
1.	76.5	550	520	3.0
2.	75.5	464	520	0
3.	74.5	513	520	0
4.	73.5	542	520	2.2
5.	72.5	535	520	1.5
6.	71.5	516	520	0
7.	70.5	512	520	0
8.	69.5	449	520	0
9.	68.5	494	520	0
10.	67.5	470	520	0
11.	66.5	470	520	0
12.	65.5	504	520	0
		Concentration = 1×10^{-4} moles/lit.		
1.	63.0	531	526	1.1
2.	63.5	540	498	2.0
3.	64.0	529	638	2.9
4.	64.5	537	520	1.7
5.	65.0	560	520	4.0
6.	65.5	548	520	2.8
7.	66.0	571	520	5.1
8.	66.2	528	520	0.8
9.	66.4	598	520	7.8*
10.	66.6	587	520	6.7
11.	66.8	564	520	4.4
12.	67.0	558	520	3.8
13.	67.8	571	520	5.1
14.	67.8	559	520	3.9
15.	68.0	571	520	5.1
16.	68.5	581	520	6.1
17.	69.0	567	520	4.7
18.	69.5	571	520	5.1
19.	70.0	579	520	5.9*
20.	70.4	571	520	5.1
21.	70.6	541	520	2.1
22.	71.0	520	520	0
23.	72.0	548	520	2.8
24.	73.0	550	520	3.0

Table 12

Variation of Absolute Count Rate with Distance

pH = 7

Concn. = .2 x 10^{-4} moles/lit.

Sl.No.	Distance	Counts/10 min.	Zero/10 minutes	Count/ minute
1.	63.0	496	507	0
2.	64.0	511	507	0.4
3.	65.0	488	507	0
4.	66.0	550	507	4.3
5.	67.0	529	507	2.2
6.	68.0	518	507	1.1
7.	69.0	526	507	1.9
8.	70.0	538	507	3.1
9.	71.0	521	507	1.4
10.	72.0	519	507	1.2
11.	73.0	509	507	0.2

Concentration = . 10^{-4} moles/lit.

1.	70.0	541	520	2.1
2.	69.0	549	520	2.9
3.	68.0	561	520	4.1
4.	67.5	503	520	0
5.	67.3	601	520	8.1
6.	67.1	618	520	9.8*
7.	66.5	563	520	4.3
8.	65.5	579	520	5.9
9.	64.5	541	520	2.1
10.	64.2	584	520	6.4*
11.	64.0	551	520	3.1
12.	63.0	539	520	1.9
13.	62.0	547	520	2.7
14.	66.0	530	520	1.0
15.	60.0	541	520	2.1

Table 13

Variation of Absolute Count Rate with Distance

pH = 8 Concn. = .2 x 10^{-4} moles/lit.

Sl.No.	Distance	Counts/10 min.	Zero/10 minutes	Count/minute
1.	0	509	536	0
2.	1	498	536	0
3.	2	539	536	0.3
4.	3	541	536	0.5
5.	4	550	536	1.4
6.	5	543	536	1.7
7.	6	519	536	0
8.	7	537	536	0.1
9.	8	503	536	0
10.	9	481	536	0
11.	10	497	536	0
		Concn. = 1 x 10^{-4} moles/lit.		
1.	0	513	501	1.3
2.	1	493	486	0
3.	2	523	500	2.3*
4.	2.6	579	500	7.9*
5.	2.8	568	500	6.8
6.	3.0	546	500	4.6
7.	3.5	531	500	3.1
8.	4.0	551	500	5.1
9.	5.0	546	500	4.6
10.	6.0	527	500	2.7
11.	6.4	558	500	5.9*
12.	6.6	549	500	4.9
13.	6.8	527	500	2.7
14.	7.0	480	500	0
15.	8.0	518	500	1.8
16.	9.0	501	500	0.1

Table 14: Percentage Hydrolysis at Different Soap Concentration |Na-My|.

S.No.	Soap concentration Molar	Fatty Acid Concn. Molar x10^{6}
1	.0001	1.8
2	.0003	3.6
3	.001	11.7
4	.005	12.5
5	.01	17.3

Table 15

Variation of 'D' with pH

pH	H^+	$K_a H^+$	K_d	$D = K_d \mid 1+K_a H^+ \mid / K_a \mid H^+ \mid$
5	10^{-5}	8.33×10^3	9.07	9.07
6	10^{-6}	8.33×10^2	5.85	5.85
7	10^{-7}	8.33×10^1	3.99	4.07
8	10^{-8}	8.33	0.845	0.946
9	10^{-9}	0.833	0.298	0.656

Table 16: Experimental Values of $\Delta \gamma_{WL} \cos \theta$.

Sl.No.	pH	Initial concn. x10^4 moles/lit.	Final concn. x10^5 moles/lit.	θ°	cos θ	γ_{WL} dynes/cm.	$\gamma_{WL} \cos \theta$ dynes/cm	$\Delta \gamma_{WL} \cos \theta$ dynes/cm
1	6.	0	0	0	1	45	45	0
2		.2	.598	144.5	-.815	33.1	-27	-72
3		.4	1.196	105.4	-.2615	32.5	-8.5	-53.5
4		.6	1.794	67.8	.378	31.0	11.7	-33.3
5		.8	2.392	61.4	.480	31.0	14.9	-30.1
6		1.0	2.990	90.0	0	29.6	0	-45.0
1	7	0	0	0	1	45	45	0
2		.16	.616	100.3	-.178	38.3	-6.8	-51.8
3		.20	.770	124.1	-.560	35.2	-19.7	-64.7
4		.40	1.54	114.6	-.415	34.8	-14.6	-59.7
5		.60	2.31	48.0	.67	34.2	22.9	-22.1
6		.80	3.08	49.0	.655	33.1	21.7	-23.3
7		1.0	3.85	79.2	.187	33.0	6.15	-38.85
1	8	0	0	0	1	45	45	0
2		.2	1.4952	138.8	-.75	33.5	-25.2	-70.2
3		.4	2.992	108.0	-.309	33.0	-10.2	-55.2
4		.6	4.484	74.1	.274	32.7	8.93	-36.05
5		.8	5.980	62.1	.4675	32.5	15.20	-29.80
6		1.0	7.476	76.0	.242	31.0	7.5	-37.50

Table 17

Comparison of Experimental and Computed Values of $\Delta\gamma_{LW}\cos\theta$

Sl. No.	pH	Initial concn. x 10^4 moles/lit	Concn. in dodecan x10^4 moles/lit	Concn. in aqueous phase x10^5 moles/lit	$\Delta\pi_{RL}$ dynes/cm.	$\Delta\pi_{RW}$ dynes/cm x10^2	$\Delta P = \Delta\gamma_{RL} - \Delta\gamma_{RW}$ dynes/cm	$\Delta\gamma_{LW}\cos\theta$ dynes/cm
1	6	0	0	0	0	0	0	0
2		.2	.351	.598	-12.4	-0.875	-12.392	-72
3		.4	.701	1.196	-24.8	-8.25	-24.710	-53.5
4		.6	1.052	1.794	-37.2	-12.5	-36.98	-33.3
1	7	0	0	0	0	0	0	0
2		.16	.296	.616	-10.5	- 1.56	-10.483	-51.8
3		.2	.308	.770	-11.18	-60.5	-11.36	-64.7
4		.4	.615	1.54	-22.58	-70.0	-21.26	-59.7
1	8	0	0	0	0	0	0	0
2		.2	.1262	1.4952	- 4.45	- 7.45	- 4.38	-70.2
3		.4	.252	2.992	- 8.90	-10.0	- 8.73	-55.2
4		.6	.379	4.484	-13.35	-33.0	-12.85	-36.05
5		.8	.505	5.980	-17.80	-55.0	-16.75	-29.8

Table 18: Effect of pH on Contact Angle, Interfacial Tension, Adsorption Density and Adhesion Tension at a Fixed Na-My Concentration.

Sl. No.	pH	Concentration of Na-My in water (moles/lit) x 10^4	Contact Angle in degrees	Interfacial tension $\gamma_{W/L}$ (dynes/cm)	Adsorption density $\Gamma_{R/W}$ (Moles x cm^2) x 10^{12}	Adhesion tension $\tau = \gamma_{L/W} \cos\theta$ (dynes/cm)
1	5	0.4	45.6	32.3	0.0	23.4
2	6	0.4	105.4	32.5	1.575	- 8.6
3	7	0.4	114.6	34.8	18.55	-14.5
4	8	0.4	108.0	33.0	16.30	-10.0
5	9	0.4	52.25	31.6	0.0	17.1

Table 19

Variation of K_D with pH

Sl. No.	Initial concn. $x10^4$	Counts/ minute after eqlm.	Corresponding amount in moles $x\ 10^7$	Amount transferred to organic phase in moles $x\ 10^7$	Distribution coefficients K_D	Mean K_D
pH = 5						
1	1.0	62	1.0	19	12.33	
2	0.75	67	1.0	14	9.1	
3	0.5	45	0.7	9.3	9.1	9.07±1
4	0.25	25	0.3	4.7	10.1	
5	0.1	12	0.15	1.95	8.0	
pH = 6						
1	1.0	128	1.9	18.1	5.85	
2	0.75	86	1.25	13.5	7.15	
3	0.5	62	1.0	9.0	5.85	5.85
4	0.25	29	0.5	4.5	5.85	
5	0.1	15	0.2	1.8	5.85	
pH = 7						
1	1.0	200	3.0	17.0	3.9	
2	0.75	134	2.4	13.0	4.23	
3	0.5	89	1.45	8.55	3.84	3.99±1
4	0.25	30	0.5	4.5	5.85	
5	0.1	6	0.1	1.9	12.33	
pH = 8						
1	1.0	560	7.8	12.2	1.04	
2	0.75	516	7.1	8.9	0.845	
3	0.5	357	5.0	5.0	0.65	0.845±0
4	0.25	230	3.0	2.0	0.42	
5	0.10	98	1.4	0.6	0.325	
pH = 9						
1	1.0	971	13.5	6.5	0.225	
2	0.75	833	11.5	3.5	0.195	
3	0.5	293	4.2	5.8	0.91	0.3±0.1
4	0.25	228	3.0	2.0	0.420	
5	0.10	80	1.3	0.7	0.351	

APPENDIX

EXPERIMENTAL ERRORS.

1.	Contact Angle Measurements	± 2°
2.	Adsorption Measurements	± 5%
3.	Distribution Coefficient	± 10%
4.	Standard Curve for PAP Adsorption	± 5%
5.	Interfacial Tension Measurements	± 2%

ERRATA

PAGE	READ	INSTEAD OF.
VIII Line8.	Bubble-Water-Tolucene	Bubble Water Tolucene
4 eqn. 2.4	S	S^4
4 26th. line	S= Total Entropy	S^4 = Surface Entropy.
5 9th. line.	all v's except v_1 and v_2	all v's except $_1$ and 1
20	Fig.2.	Fig. 9.
21	Fig. 3.	Fig. 10.
22	Fig. 4.	Fig. 2.
24	Fig. 5.	Fig. 3.
25	Fig. 6.	Fig.4.
27	Fig. 7.	Fig.4
30	Fig.8.	Fig. 6.
31	Fig9.	Fig.7.
35	Fig.10.	Fig. 11.

At all the places the corrected Fig. Nos. have to be read.